Hail occurrence in the Napf region in Switzerland

Master Thesis

Faculty of Science

University of Bern

handed in by

Ursina Schwyn

2022

Supervisor

Prof. Dr. Olivia Romppainen-Martius

Institute of Geography, Mobiliar Lab for Natural Risks and

Oeschger Centre for Climate Change Research

University of Bern

Co-Supervisor

Dr. Katharina Schröer

Institute for Environmental Decisions, ETH Zürich and

Federal Office of Meteorology and

Climatology MeteoSwiss

Abstract

Hail is one of the costliest natural hazards in Switzerland and across central Europe. Due to the small spatial and temporal scales, the high natural variability in hailstone sizes and a lack of long-term ground observation systems, no hail climatology was available in Switzerland prior to 2016. In 2016, the first scientific climatological analysis was published. From 2018 to 2021, a uniform national reference on hail hazards was developed. This hail climatology project is based on data from the Swiss weather radar network and was developed within the framework of the National Centre for Climate Services, NCCS. The Napf region is a hail hot spot in Switzerland. However, the mechanisms behind the local frequency maximum in the Napf region are not well understood and are currently not fully reproduced by the environmentallyddriven resampling models developed in the hail climatology project.

Here, this master thesis aims to contribute to a better understanding of conditions and processes leading to hail in the Napf region. The results show that the relative frequency is with 5 % twice as high as in the Albis region or the whole of Switzerland, which served as reference regions. The hail cells crossing the Napf region were categorized into the locally-triggered hail cells and the imported hail cells from other regions. The environmental conditions were then analyzed using ERA5 data, and compared for the different categories. A flat pressure distribution and low wind shear are present on days where locally-triggered cells occur. The flow situation is generally dynamical on days where imported hail cells occur. To investigate local phenomena in more detail, 26 case studies were conducted by using COSMO data. Unfortunately, no new findings could be detected in the case studies, but the case studies represent the results found by the ERA5 analysis very well.

Contents

List of Abbreviations

CAPE ..... Convective available potential energy
CIN ..... Convective inhibition
COSMO ..... Consortium for Small-Scale Modelling
DWD ..... Deutscher Wetterdienst
ECMWF ..... European Center for Medium-Range Weather Forecast
ET ..... Echo Top
GWT ..... GrossWetterType
GWTWS ..... GrossWetterTypeWS
IFS ..... Integrated Forecast System
MESHS ..... Maximum Expected Severe Hail Size
MSL ..... Mean Sea Level Pressure
NCCS ..... National Centre for Climate Services
NWP ..... Numerical Weather Prediction
POH ..... Probability of Hail
TRT ..... Thunderstorm Radar Tracking

1 Introduction

Hail is one of the costliest natural hazards in Switzerland and across central Europe (BAFU Bundesamt für Umwelt, 2016; VKF, 2013; Lellig et al., 2014; Mohr et al., 2015a). On 23 July 2009; severe thunderstorms with hail reached Switzerland from the south-west and crossed the Swiss Plateau and the Pre-Alps. These storms were one of the costliest hail events in Swiss history due to the damage they caused. The enormous damage is on the one hand due to the extraordinary long lifetime of the two daughter cells arising from the main storm of 4 hours. On the other hand, the area affected was 10,000 km^2, which is a quarter of the size of Switzerland. The maximum hailstone sizes were 5 to 6 cm in diameter (NCCS National Center for Climate Services, 2021; Sturmarchiv Schweiz, 2019a,b). The total losses in agriculture, buildings, and vehicles added up to over CHF 600 million (Torriani-Braga, 2009).

The large damage potential associated with hail is well known. Due to the small spatial scale of hail, the spatial variability in hailstone sizes and a lack of long-term ground observation systems, Switzerland did not have a hail climatology prior to 2016. In 2016, the first scientific climatological analysis was published (Nisi et al., 2016). From 2018 to 2021, a spatially explicit uniform national reference on hail hazards was developed based on the Swiss weather radar network. This project was realized within the framework of the National Centre for Climate Services (NCCS). Marked regional differences are shown by the hail frequency patterns. In the "Hail Climate Switzerland" project, the following products were made available: information on the hailstone size, hail frequency and return periods. These products are accessible for the measurement period since 2002 on a monthly and annual basis. Additionally, hail hazard maps are provided that give a very precise data basis in terms of time and location for the assessment of the risk of hail damage in all regions of Switzerland (NCCS, 2021; MeteoSwiss, 2021).

Deep, moist convection needs the following three ingredients (Doswell III et al., 1996; Johns and Doswell, 1992; Doswell, 1987): (a) high amounts of moisture in the lower

troposphere, (b) unstable atmosphere and (c) lifting of a parcel to reach its level of free convection (LFC) and release the atmospheric instability. These ingredients are all necessary, but not always sufficient for the development of convective storms. According to Johns and Doswell (1992), convective storms are considered "severe" if the hail diameter exceeds 1.9 cm. When high amounts of moisture, an unstable atmosphere and a lifting mechanism are present simultaneously, vertical wind shear may reinforce convection and render it severe (Kaltenböck et al., 2009; Weisman and Klemp, 1984; Wallace and Hobbs, 2006). The vertical wind shear influences the lifetime of storms; it is needed to form multicell and supercell storms as it leads to the separation of up- and downdraft regions (Davies and Johns, 1993; Bluestein, 1993).

In the United States, severe convection requires large values of convective available potential energy (CAPE) (Madonna et al., 2018). Brooks et al. (2007) found that during a large period of time during the year the climatological conditions support severe thunderstorms in the US. In Europe, on the other hand, his results suggest that synoptic and mesoscale conditions are required to get environmental conditions supportive of the most severe convection. Especially the interaction between orography and the synoptic flow, as well as mesoscale conditions like fronts are very important factors for the development of hail in Europe (Madonna et al., 2018; Kunz and Puskeiler, 2010). As a result, forecasters in Europe will have an additional challenge in the forecast process as they are unlikely to find widespread regions associated with severe convective environments as it is the case in the US (Brooks et al., 2007). In Switzerland, most hail events are observed in the pre-Alpine regions north or south of the Alps (Nisi et al., 2016).

Generally, favorable conditions for severe convective storms are set up by large-scale flow (Nisi et al., 2016; Schemm et al., 2016; Doswell, 1987) – according to Schemm et al. (2016) 20% to 40% of the hailstorms observed in Switzerland form in pre-frontal environments. Nisi et al. (2018) as well as Schemm et al. (2016) found that West and South-West circulation types are most frequently linked to hail events in Switzerland.

Furthermore, complex topography can influence convective events severely, for example, by thermo-topographic wind systems triggering convective cells (Trefalt et al., 2018). Nisi et al. (2016) suggest that orographic forcing mechanisms and related flow convergence are decisive for hailstorm development in Switzerland. In those regions warm and moist air is forced to lift due to low-level convergence. These convergence zones can be caused by the flow deviations at the hills, by the outflow of previously developed thunderstorm cells in alpine valleys, or by flow-around regimes (Nisi et al., 2016). de la Torre et al. (2015) discussed the role of flow anomalies caused by topography for the formation of severe thunderstorms of the Southern Andes. Punge and Kunz (2016) did a review of hail observations and hailstorm characteristics including over 40 studies, mainly performed in Europe. Punge and Kunz (2016) indeed found evidence for a relationship between orography and hailstorm or hail frequency. Trefalt et al. (2018) state that there are few detailed studies of the role of orography for hail in Switzerland.

The spatial variability in hail occurrence is high in Switzerland (Barras et al., 2019). This high variability is often caused by specific terrain characteristics, which trigger most of the hail events in Southwest Germany (Kunz and Puskeiler, 2010). The local phenomena of hail in the Alpine region can only be studied by accounting for the interplay between the synoptic flow and the complex orography (Kunz and Puskeiler, 2010). Many studies do not take a closer look at this very important interplay because it complicates the triggering mechanisms even more. One example for neglecting the local-scale forced ascent induced by complex orography is the logistic hail model for Germany developed by Mohr et al. (2015b).

This situation motivated me to study hail events in more detail in Switzerland. I did that by taking a climatological perspective on the regional-to-local patterns of hailstorm occurrence in a hail-prone region in Switzerland, namely the Napf region. The Napf region is a hail hot spot in Switzerland (Nisi and Stoll, 2021; MeteoSwiss, 2021; NCCS, 2021). The hot spot can either be due to an increased number of thunderstorms overall, or due to an increased relative frequency of hailstorms compared to

thunderstorms.

My main data source is radar hail data. Because there are generally high uncertainties associated with hail in observations, I complement the quantitative analysis of the radar hail data with local expert knowledge from professional forecasters. The aim of this thesis is to analyze and compare observed hailstorm tracks that occurred in the Napf region, and to explore typical conditions that lead to different hailstorm patterns. Interviewing professional forecasters helps to better understand potential triggering mechanisms for hail cells and include them into the analyses. This study considers atmospheric variables, triggering mechanisms, and the cells' hailstorm characteristics. Five hailstorm characteristics that can be quantified for each hail cell are (1) area, (2) lifetime, (3) maximum expected severe hail size, (4) bearing, and (5) path length. The three research questions are the following:

- *[A] Why is the frequency of hail days higher in the Napf region? – Are the hail cells locally triggered or pre-existing and thus "imported" from other regions?*
- *[B] What is the magnitude of the above-mentioned hailstorm characteristics for hail events that occur in the Napf region?*
- *[C] Under which mesoscale conditions do hail events occur in the Napf region?*

Answering these questions helps to better understand hailstorms that affect the Napf region, and possibly other parts of the country as well.

Following this chapter a description of the data (section 2), and the methods (section 3) used in this master thesis are presented. Subsequently, in chapter 4, the results are presented and they are discussed to answer the research questions in chapter 5. The conclusions follow in chapter 6, followed by a short outlook in chapter 7.

2 Data

Radar hail data (subsection 2.2) is used to distinguish thunderstorm cells from hail cells. Thunderstorm track data generated by the thunderstorm radar tracking (TRT) algorithm (subsection 2.3), combined with radar hail stone size footprints (subsection 2.4) to follow the tracks of hail cells. To investigate the environmental conditions, ERA5 reanalysis data (subsection 2.6), as well as COSMO analysis data (subsection 2.7) is used. Information about the weather conditions is included by using preclassified weather types (subsection 2.5).

2.1 The Napf Region

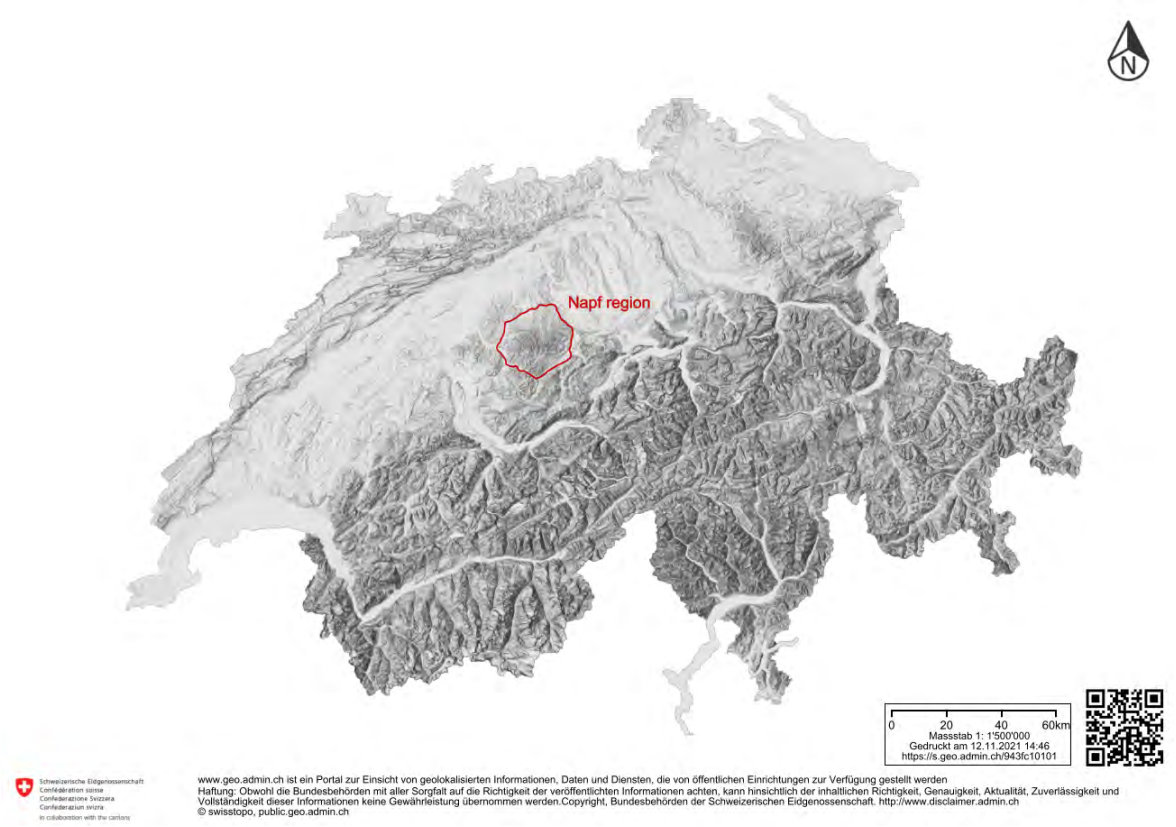

Figure 1: The Napf region in the national context of Switzerland, the grey shading represents the topography of Switzerland. Use the QR code to get to the map.geo.admin website. Source: map.geo.admin.ch

The Napf peak, with an altitude of 1406 masl, is the highest peak between the Bernese Emmental and the Lucerne Entlebuch. The Napf region reaches from the peak to the Emme valley (German: Emmental) in the Southwest, and to the Entlebuch in the Southeast (Figure 2). In the Northeast the Napf region is bound by the municipalities of at Wilisau, Metznau and Wolhusen. In the Northwest the Napf region ends at the municipalities of Sumiswald, Dürrenroth and Huttwil.

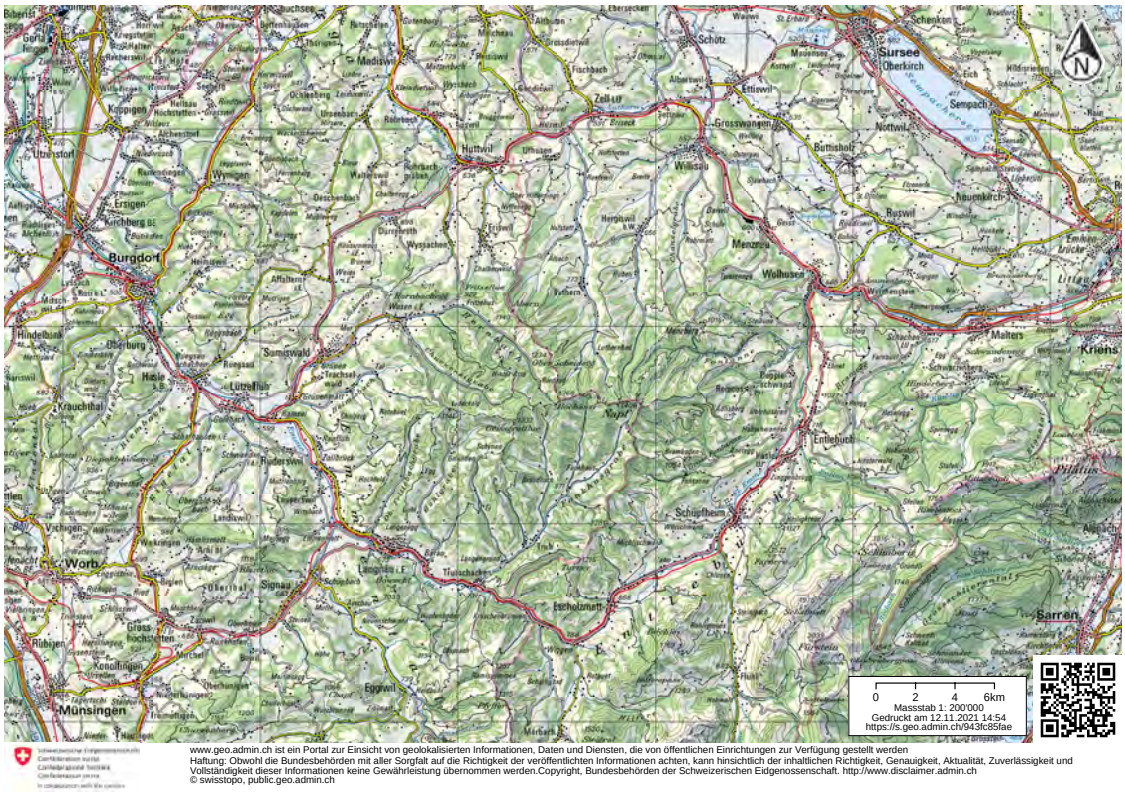

Figure 2: The Napf region is in the center of the map, communities and valleys that confine the Napf region around. Use the QR code to get to the map.geo.admin website. Source: map.geo.admin.ch

The Napf region is known as a hail hot spot, with above-average hail frequency. Figure 3 shows the the average number of hail days per km^2 in the summer half-year over whole Switzerland. In the Ticino, the Jura Mountains and Central Switzerland, a high average number of hail days can be observed. The Napf region is located in the greater Central Swiss region and is marked by a red circle. Regions which show a high number of hail days consequently have a high hail frequency.

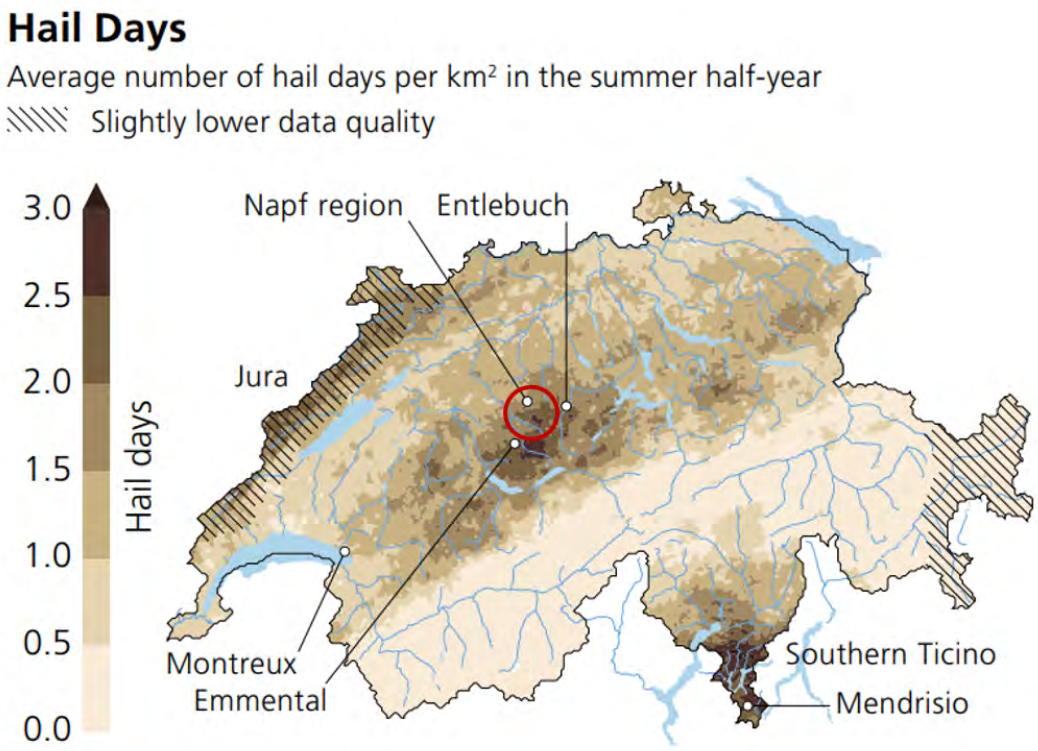

Figure 3: Average number of hail days per km^2 from April to September. Increased hail frequency in the Ticino, the Jura Mountains, and Central Switzerland. The Napf region with its increased hail frequency is depicted by the red circle. Source: NCCS brochure «Hail Climate Switzerland»

2.2 Radar Hail Data: POH and MESHS

The Probability of Hail (POH) (Waldvogel et al., 1979; Witt et al., 1998) and the Maximum Expected Severe Hail Size (MESHS) (Treloar, 1998; Joe et al., 2004) are two radar-based hail detection products. POH indicates the probability of hail reaching the ground, on a range from 0% to 100%. MESHS provides an estimation of the maximal hailstone size on the ground, with smallest values of 20 mm (Nisi et al., 2016; Trefalt et al., 2018). Thanks to the high spatiotemporal resolution (1km x 1km, 5 min) of radar measurements, radar-based statistics have good accuracy and are widely used for nowcasting and research purposes (Nisi et al., 2016; Barras et al., 2019).

POH and MESHS have already been validated with insurance loss data and crowd sourcing in earlier studies by Nisi et al. (2016) and Barras et al. (2019). The main findings of the validations are a general overestimation of the grain size by the MESHS

algorithm (Barras et al., 2019), and a reliable threshold for the presence of hailstones at the ground for $POH \geq 80\%$ (Nisi et al., 2016).

POH is computed at MeteoSwiss following the method of Waldvogel et al. (1979) and Foote et al. (2005). The 45 and 50 dBz echo top height products are used (ET45 and ET50) to calculate the POH and MESHS. ET45 and ET50 are the highest altitudes at which a radar reflectivity of minimum 45 and 50 dBz, respectively, can be detected. Further, POH and MESHS need information on the freezing-level-height (H0). The freezing-level-height information is taken from the COSMO model analysis (Nisi et al., 2016).

2.3 Thunderstorm Radar Tracking (TRT)

The thunderstorm radar tracking (TRT) algorithm has been in service at MeteoSwiss since 2004. It is used for nowcasting and research purposes Hering (2018). The TRT algorithm identifies cells as thunderstorm cells if their reflectivity exceeds a certain threshold, depending on the stage of the cell's life cycle (36-48 dBZ). This makes it possible to track mature systems and detect potentially severe thunderstorms. The identified thunderstorm cells can be single cells or also multicell cluster in time and space, consisting of a group of cells moving as a single unit (Trefalt, 2017; Hering, 2018). For more information on the TRT algorithm, please refer to Hering et al. (2004), Hering et al. (2008) or Rotach et al. (2009).

2.4 Footprints

In my thesis, the main source for radar hail data are the MESHS footprints. An example footprint is shown in figure 4. MESHS footprints are hailstorm footprints that combine the MESHS 5-min radar hail data with the TRT-outline information of the storm cells. These hailstorm footprints are provided by MeteoSwiss and have been created for the project called "National Hail Climatology Switzerland". The MESHS footprints allow researchers to take a detailed look at how individual hailstorms evolve

and see what the spatial MESHS patterns are within those storm cells. Due to the 5 minute resolution of the footprints, the location of where a thunderstorm becomes a hailstorm can be detected. Table 1 lists the investigated variables for each hail cell. This is a list of all variables used in this analysis.

Parameter	**Explanation**	**Unit**
Storm-ID	Each storm has a unique ID	-
First Detection	Date and Time of storm first detection	-
Last Detect	Date and time of storm decay	-
path length	Track length of each storm cell	[km]
area	Area of each storm cell	[km^2]
lifetime	Lifetime of each storm cell	[min]
max MESHS	maximal measured MESHS	[mm]
MESHS	MESHS for each 5 min step for the entire storm life cycle	[mm]

Table 1: Variables used from the footprint data set for each storm cell.

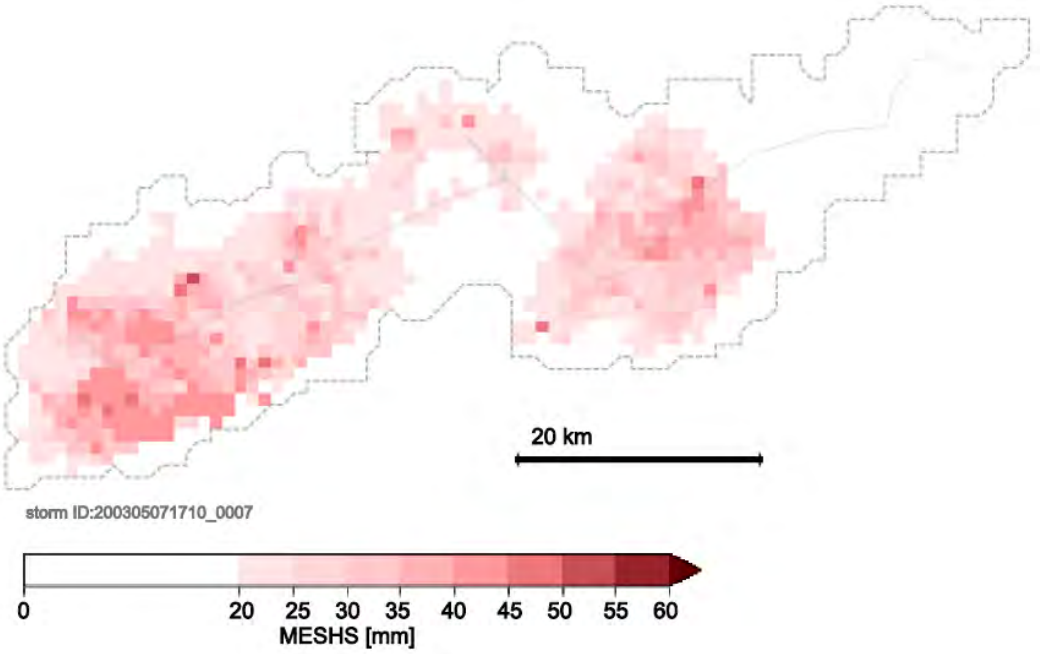

Figure 4: Example footprint, of a hailstorm cell that occurred on May 8th 2003. The reddish colors show the MESHS, grey line in the middle is the trajectory, and the grey outline shows the area affected by the hailstorm as detected by the TRT-algorithm. Source: MeteoSwiss

2.5 Weather Types

A weather type classification by MeteoSwiss is used to get a first overview of the synoptic weather conditions (Weusthoff, 2011). The classification identifies weather patterns for Central Europe. In this thesis, a classification method which is based on geopotential height is used. This classification has eleven types and is named GrossWetterTypeWS (GWTWS). GWTWS is based on the GrossWetterType (GWT) classification using 500 hPa geopotential height as input data. GWTWS divides the synoptic weather conditions into eight wind directions (GWT classification), and low, high or flat pressure distributions. To determine low, high or flat pressure distributions, GWTWS additionally uses the mean wind speed at 500 hPa to differentiate convective and advective situations applying the threshold of 7 m/s. For advective situations (wind speed $>$ 7 m/s), the weather type derived by the 8 types GWT classification is used. For convective situations (wind speed $<$ 7 m/s), the mean sea level pressure (MSL) averaged over the chosen domain is an indicator for low (MSL $\leq$ 1010 hPa), high (MSL $\geq$ 1015 hPa) and flat (1010 hPa $<$ MSL $<$ 1015 hPa or wind speed $<$ 3 m/s) pressure distributions (Weusthoff, 2011).

GWTWS is computed from European Center for Medium-Range Weather Forecasts (ECMWF) ERA-Interim reanalysis data from 2002-2010. Since 2011 it is calculated from operational ECMWF Integrated Forecast Systems (IFS) data (Weusthoff, 2011).

2.6 Reanalysis Data: ERA5 Data

Reanalysis data are used to get an overview over the mesoscale conditions, in addition to the weather types. Reanalysis data provide a very complete picture of past weather and climate. They are a blend of observations with past short-range weather forecasts rerun with modern weather forecasting models (ECMWF, 2021).

ERA5 reanalysis data is used of a 6-hourly temporal resolution and 0.25 x 0.25° spatial resolution which corresponds to 31km^2 at 47°N. The data covers a time period from 1950 until today (Hersbach et al., 2020). The variables used for this analysis are summarised in Table 2. CIN values were found to have missing values and therefore

may need to be treated with caution. In addition to the variables listed in table 2, wind speeds and the vertical wind shear were calculated from the ERA5 data, see table 3. The vertical wind shear was calculated using the 850 to 500 hPa bulk wind shear. The bulk wind shear is represented by the vector difference between 500 hPa and 850 hPa (Bunkers, 2002). This method to calculate the vertical wind shear was chosen because the wind vectors are not available at any pressure level between 500 and 850 hPa. Hence, a cumulative calculation of the vertical wind shear is not possible.
The ERA5 data were provided by MeteoSwiss.

Parameter	**Level [hPa]**	**Explanation**	**Unit**
u	500, 850	Zonal velocity of the wind	[m/s]
v	500, 850	Meridional velocity of the wind	[m/s]
cape	-	Convective available potential energy	[J/kg]
cin	-	Convective inhibition	[J/kg]
t2m	-	2 metre temperature	[K]
z	500, 850	Geopotential	[m^2/s^2]

Table 2: Variables used from the ERA5 dataset

Parameter	**Level [hPa]**	**Explanation**	**Unit**
Wind speed	500, 850	$\sqrt{u^2 + v^2}$	[m/s]
Bulk wind shear	850 - 500	$\sqrt{(u850 - u500)^2 + (v850 - v500)^2}$	[m/s]

Table 3: Variables calculated from the ERA5 dataset variables.

2.7 NWP Data: COSMO Analysis Data

The COSMO-model is a non-hydrostatic atmospheric prediction model (Doms and Baldauf, 2021). A non-hydrostatic model does not make the hydrostatic assumption, so that the vertical momentum equation is solved. This allows non-hydrostatic models to be used for small horizontal scales, resolving meso-β and meso-γ scale circulations such as cumulus convection. Additionally, the impact of topography on the formation of convection is represented very realistically in non-hydrostatic forecast models (AMS, 2021).

The COSMO-model is not only used for various scientific applications but also for operational numerical weather prediction (NWP) at different meteorological services as for example MeteoSwiss, Deutscher Wetterdienst (DWD) or at the National Meteorological Administration in Bukarest, Romania. The ensuing developments related to the COSMO-Model have been organized within "COSMO", the Consortium for Small-Scale Modelling (Doms and Baldauf, 2021; AMS, 2021). The COSMO data are very useful because local scale processes can be captured due to the 1km spatial resolution. I use hourly temporal resolution of the COSMO data, provided by MeteoSwiss. The hourly temporal resolution allows me to observe the evolution of different variables during hail events as for example CIN, the bulk wind shear, or the wind speed. Since the COSMO data needs to be interpreted manually for each hailstorm, only selected case studies were analyzed. The COSMO variables used are summarised in table 4. Based on the variables in table 4, the bulk wind shear and divergence were calculated, see table 5.

Parameter	**Level [hPa]**	**Explanation**	**Unit**
FF	500, 850	Wind speed	[m/s]
u	850	Zonal velocity of the wind	[m/s]
v	850	Meridional velocity of the wind	[m/s]
CAPE_MU	-	CAPE of most unstable parcel	[J/kg]
CIN_MU	-	CIN of most unstable parcel	[J/kg]
T_2M	-	2m air temperature	[K]
HZEROCL	-	2m dew point temperature	[K]
RELHUM	500, 850	Relative humidity	[%]
HPBL	-	Boundary layer height	[m]

Table 4: Variables used from the COSMO dataset

Parameter	**Level [hPa]**	**Explanation**	**Unit**
Bulk wind shear	850 - 500	$\sqrt{(u850 - u500)^2 + (v850 - v500)^2}$	[m/s]
Divergence	850	use the metpy.calc.divergence function in python	[s^{-1}]

Table 5: Variables calculated using the COSMO variables.

3 Methods

In addition to quantitative data analyses of radar hail and environmental data, I used a blended approach that includes conducting expert interviews with forecasters.

3.1 Interview

Very little is known about the specific weather dynamics that play a role for triggering hailstorms in the Napf region and make it a hot spot region. Therefore, it is one opportunity to leverage existing knowledge and talk to experts in this field to learn what they observed in the past years. The interview was set at a very early stage in the process to get an overview and profit from the experts' knowledge. The hypotheses that resulted from the conversation were then the guidelines for my further research. The interview with Marco Stoll and Luca Nisi (both from MeteoSwiss) was held in the form of a semi-structured interview (Adams, 2015). Semi-structured interviews use a blend of closed- and open-ended questions. The questions are often accompanied by follow-up *how* or *why* questions (Adams, 2015). The transcript can be found in the appendix.

3.2 Data Processing

For this thesis, the main source for radar hail data are the MESHS footprints, as mentioned in subsection 2.4. In order to analyze the Napf-specific patterns of hail in this hot spot region, the MESHS footprints needed to be processed for further usage. This was done in four steps (see Table 6). First, the initial dataset was reduced by removing all cells with a lifetime of fewer than 15 minutes. Second, all cells, which did not cross the Napf region[1] during their lifetime were removed . This results in 515 hail cells that cross the Napf region, last for at least 15 minutes and have a MESHS of at least 20 mm at some time. Third, I removed all cells which did not produce hail over the Napf region, which left 279 cells. Fourth, these cells were then separated into three categories according to their initiation location, and the location of their first MESHS

[1]With this link you can download the shape file of the Napf region: https://www.dropbox.com/sh/7n5m13kmywnunq6/AADRFfjkA7mO85JqSs9vZP1ra?dl=0

signal. Due to this categorisation, locally triggered hail cells in the Napf region and imported hail cells from other regions can be differentiated. The imported hail cells from other regions can further be separated into hail cells that hailed over the Napf region, but also showed hail signals already outside the Napf region and hail cells that became hailstorms as they crossed the Napf region (they were ordinary thunderstorm cells before that). This separation allows me to compare the environmental conditions, as wind speed or the bulk wind shear, for the three categories. Figure 5 shows the initiation location of the 279 hail cells producing hail in the Napf region. Category 1 includes all hail cells that were initiated in the Napf region. The grey circle depicts the Napf region. Category 2 includes all hail cells that were initiated outside the Napf region but the first MESHS signal was located in the Napf region (the MESHS signal is not shown on Figure 5). Category 3 includes all hail cells that initiated outside the Napf region and also their first MESHS was outside the Napf region.
This classification can be summarized as follows:

- *Category 1:* Hail cells that were triggered in the Napf region.
- *Category 2:* Hail cells that were not triggered in the Napf region, but which became hailstorms as they crossed the Napf region (they were ordinary thunderstorm cells before that).
- *Category 3:* Hail cells that hailed over the Napf region, but also showed hail signals already outside the Napf region.

	Remaining cells	Category 1	Category 2	Category 3
Total number of hail cells (HC)	32'714			
HC crossing Napf region (NR)	515			
HC with hail signal over NR	279			
Categorisation		99 (79)	53 (45)	127 (99)

Table 6: Number of hailstorm cells after each data processing step. In brackets are the total number of days on which the storms were observed.

Figure 6 (a) depicts the trajectories of the category 1 hail cells. Figure 6 (b) shows the trajectories of the category 2 hail cells and Figure 6 (c) depicts the trajectories of the category 3 hail cells.

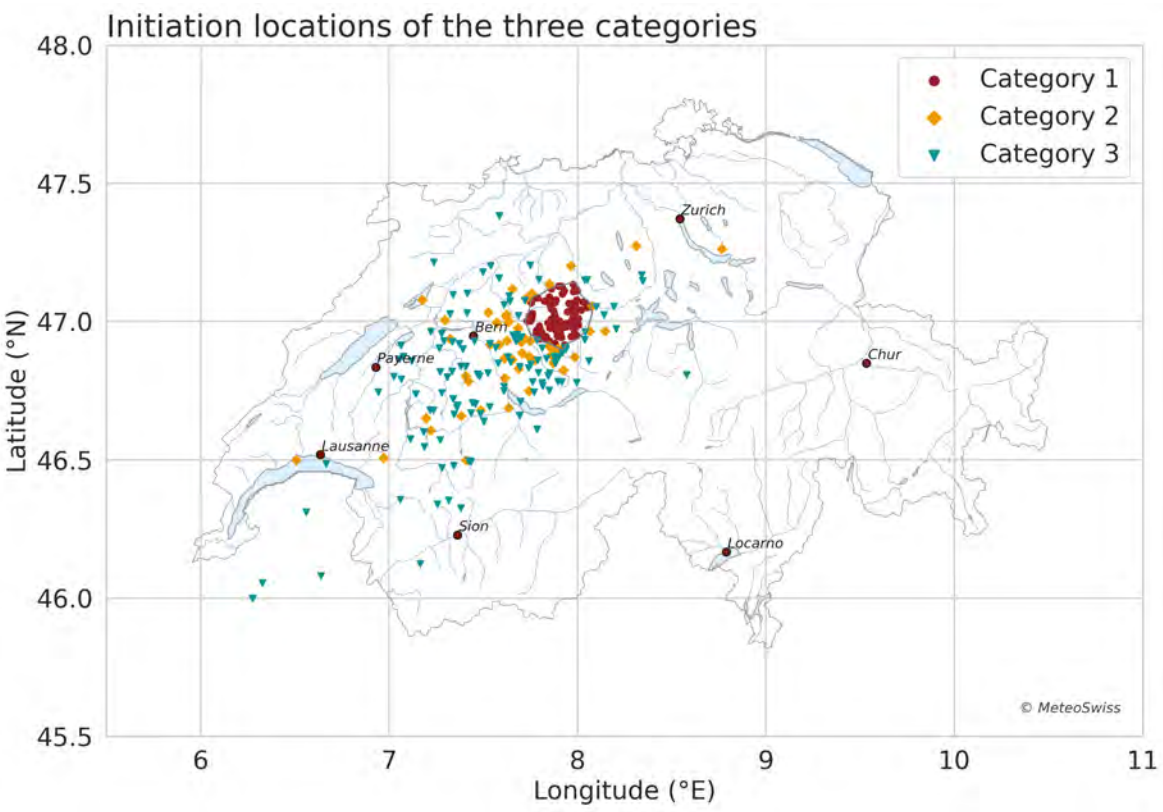

Figure 5: Initiation locations of all 279 hail cells crossing the Napf region, the grey circle depicts the Napf region.

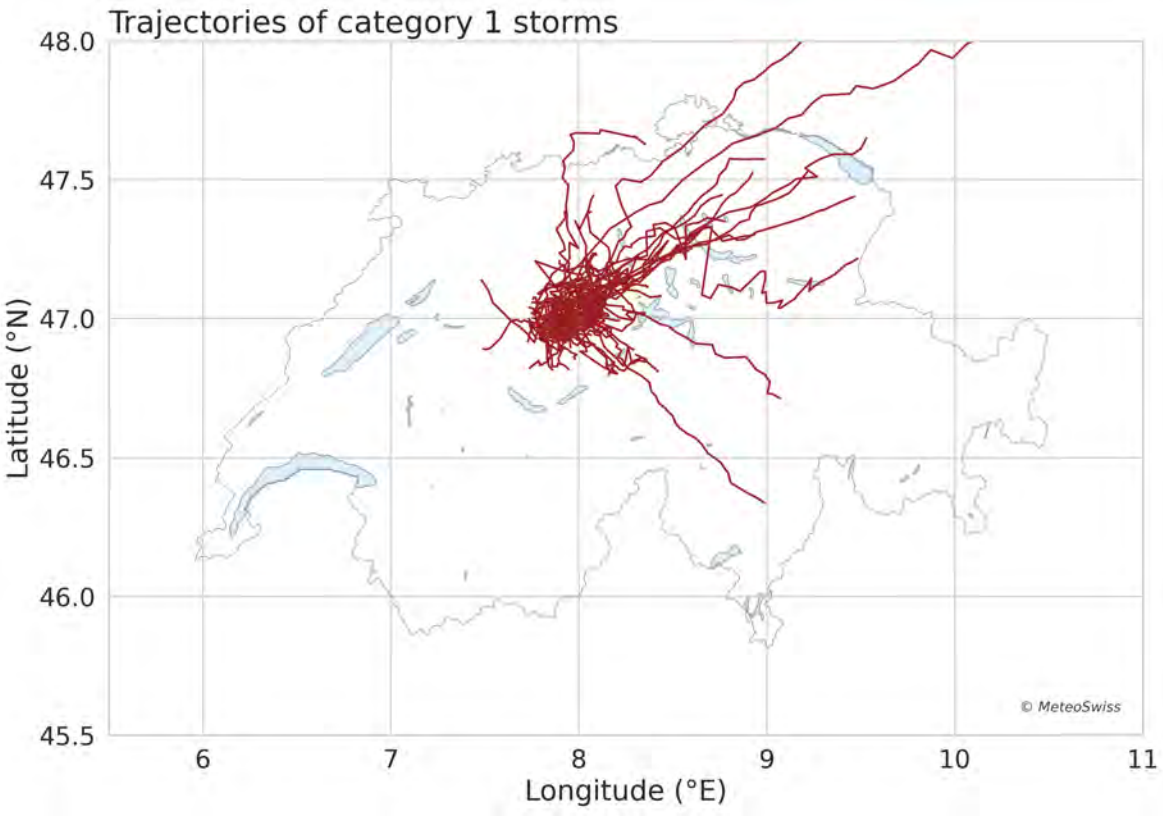

(a) Trajectories of the 99 category 1 hail cells.

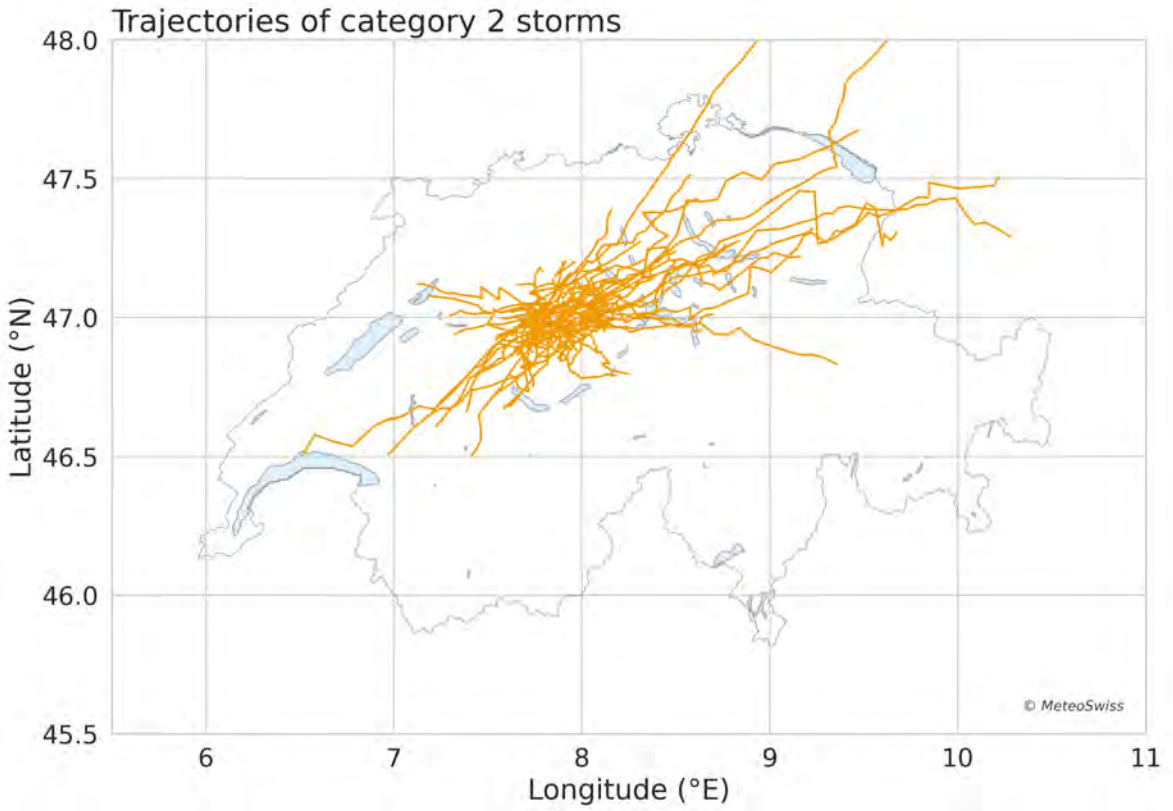

(b) Trajectories of the 53 category 2 hail cells.

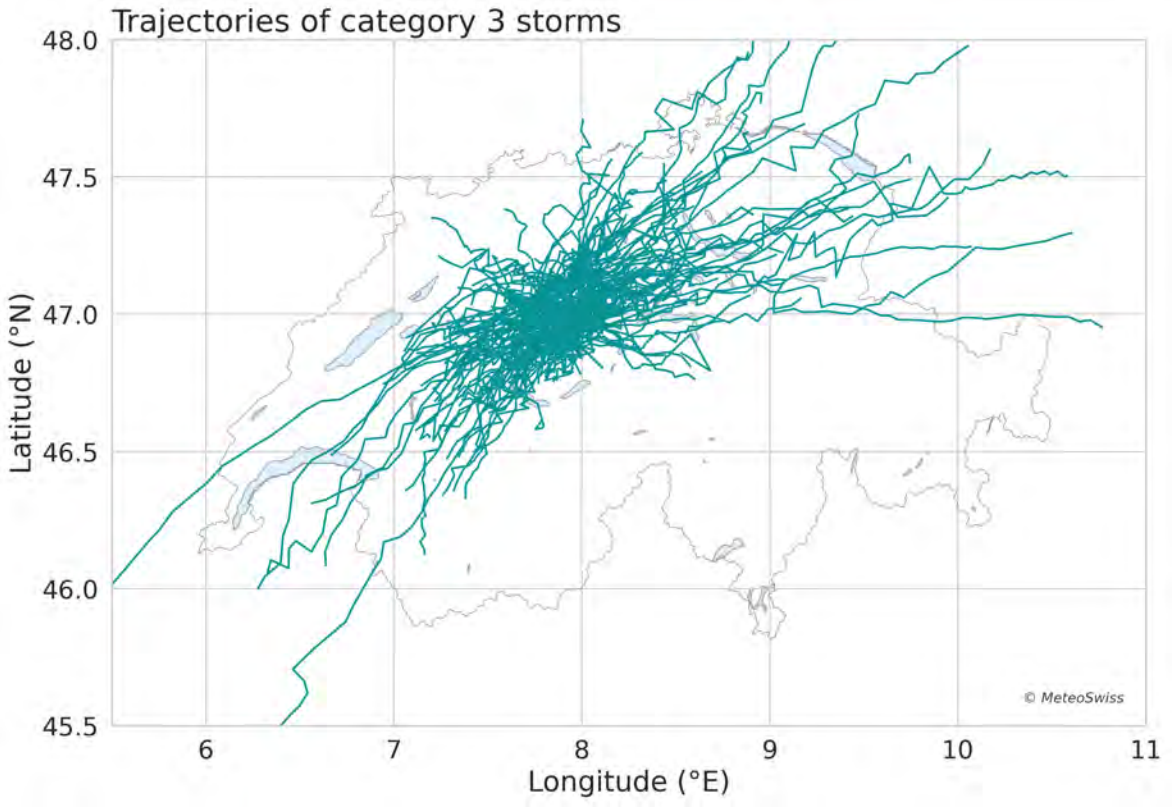

(c) Trajectories of the 127 category 3 hail cells.

Figure 6: Trajectories of the 279 Napf hail cells according to their category.

3.3 Relative Frequency Analysis

As introduced in section 1, there are two possibilities why the Napf region is a hail hot spot. The first one is that the absolute number of thunderstorms is higher in the Napf region, and therefore also the absolute number of hailstorms. The second possibility is that the absolute number of thunderstorms is not increased, but the absolute number of hailstorms is. To test this, a relative frequency analysis was carried out for the Napf region. The same analysis was also carried out for the Albis region[2] and whole Switzerland to compare to.

3.4 Category Analyses

In addition to the three categories introduced in subsection 3.2, two reference categories were formed, namely categories 4 and 5. Category 4 includes all days of the hail season (April to September), on which no hail was observed in Switzerland. Category 5 consists of all days on which hail cells were observed in Switzerland, but not in the Napf region.

3.4.1 ERA5 Box Plot Analysis

In chapter 4.4 it was found that the data becomes more robust and the yearly cycle becomes clearer by eliminating the first and the last month of the hail season, namely April and September. This is the reason why the box plot analysis was performed with May to August data only.

For the box plot analysis, the 12:00 UTC ERA5 data was extracted for May to August. The corresponding days for each cluster were taken. These daily values were then averaged over the area of the cantons Fribourg, Bern, and Lucerne[3] (Figure 7) for category 2 and 3 hailstorms. This region was taken because the most of the category 2 and 3 hailstorms were triggered in this region. For category 1, the 12:00 UTC ERA5 data was averaged over the Napf region as these cells were locally triggered.

[2]With this link you can download the shape file of the Albis region: https://www.dropbox.com/sh/7n5m13kmywnunq6/AADRFfjkA7mO85JqSs9vZP1ra?dl=0

[3]With this link you can download the Fribourg-Bern-Lucerne shape file: https://www.dropbox.com/sh/7n5m13kmywnunq6/AADRFfjkA7mO85JqSs9vZP1ra?dl=0

In addition to the 3 categories, also reference categories 4 and 5 were included in the analysis. Analogous to categories 2 and 3, also for reference categories 4 and 5, the 12:00 UTC ERA5 data was averaged over the area of the cantons Fribourg, Bern and Lucerne.

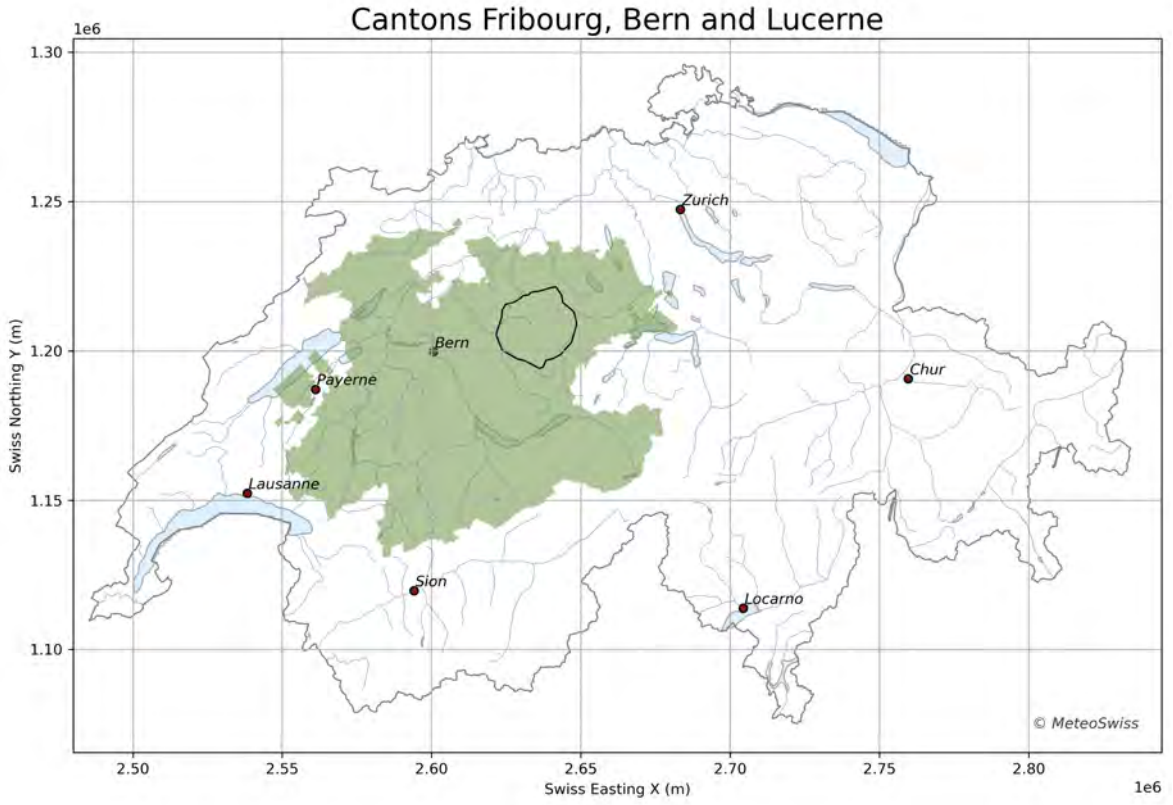

Figure 7: Area of the cantons Fribourg, Bern, and Lucerne combined in green.

3.4.2 ERA5 Composite Analysis

To get a spatial overview of the meso-scale weather pattern I produced 2D composite maps. As input data the 12:00 UTC data of the corresponding days for each cluster were taken for May to August. For each grid point the median of the values on all the corresponding days of each category were taken.

3.5 Case Studies

COSMO provides hourly analysis data with a resolution of 1km. This is connected with enormous data sets and therefore not all 279 hailstorms can be investigated using the COSMO data. Hence, a selection of case studies is necessary.

I selected 6 to 9 hail days of each category for the case study, based on the procedure below. 9 hail days for category 1, 6 hail days for category 2 and 8 hail days for category 3. The 9 category 1 hail days include 11 category 1 hailstorms (Figure 8 (a)), the 6 category 2 hailstorms include 7 category 2 (Figure 8 (b)) hailstorms and the 8 category 3 days include 8 category 3 hailstorms (Figure 8 (c)). It was the goal of the selection to choose days on which hailstorms of only one category occurred. If storms of multiple categories occurred, then this day has good conditions for the initiation of storms belonging to different categories. Therefore, an attribution of the environmental conditions to one storm is almost impossible.

The hail days were chosen according to the hailstorms that happened on the respective days. For the selection of the hailstorms I chose hailstorms that are not outliers in the respective category, but lie always close around the median in terms of path length and lifetime. Further, I checked the Sturmarchiv and looked up which days hailstorms were observed in the Napf region (Sturmarchiv Schweiz, 2021). The Sturmarchiv is the Swiss severe weather database. This is an important step as the footprints rely on radar data only and thus deliver no proof that hail was observed in the Napf region for the 279 hail cells that resulted from the data processing in section 3.2. For the case studies days I considered hailstorms of 2013 or more recent years, since COSMO data is only available from this time onwards. As a last criterion, I only considered hailstorms occurring from May to August. The reason for this filtering will be explained in the results section 4.4.

This process results in a total of 23 case study days and 26 case study hailstorms. The exact dates for the case studies are listed in Table 7.

Category 1 hail days	Category 2 hail days	Category 3 hail days
2016-06-07	2016-06-15	2016-06-24
2016-08-16	2018-05-30	2016-06-30
2017-06-02	2018-08-08	2017-25-12
2017-08-24	2019-07-06	2017-07-10
2018-05-18	2020-07-28	2017-07-21
2018-05-27	2020-08-17	2017-07-22
2018-05-31	-	2017-08-01
2020-07-02	-	2017-08-18
2020-08-13	-	-

Table 7: Date of the hail days chosen for the case studies. (YYYY-MM-DD)

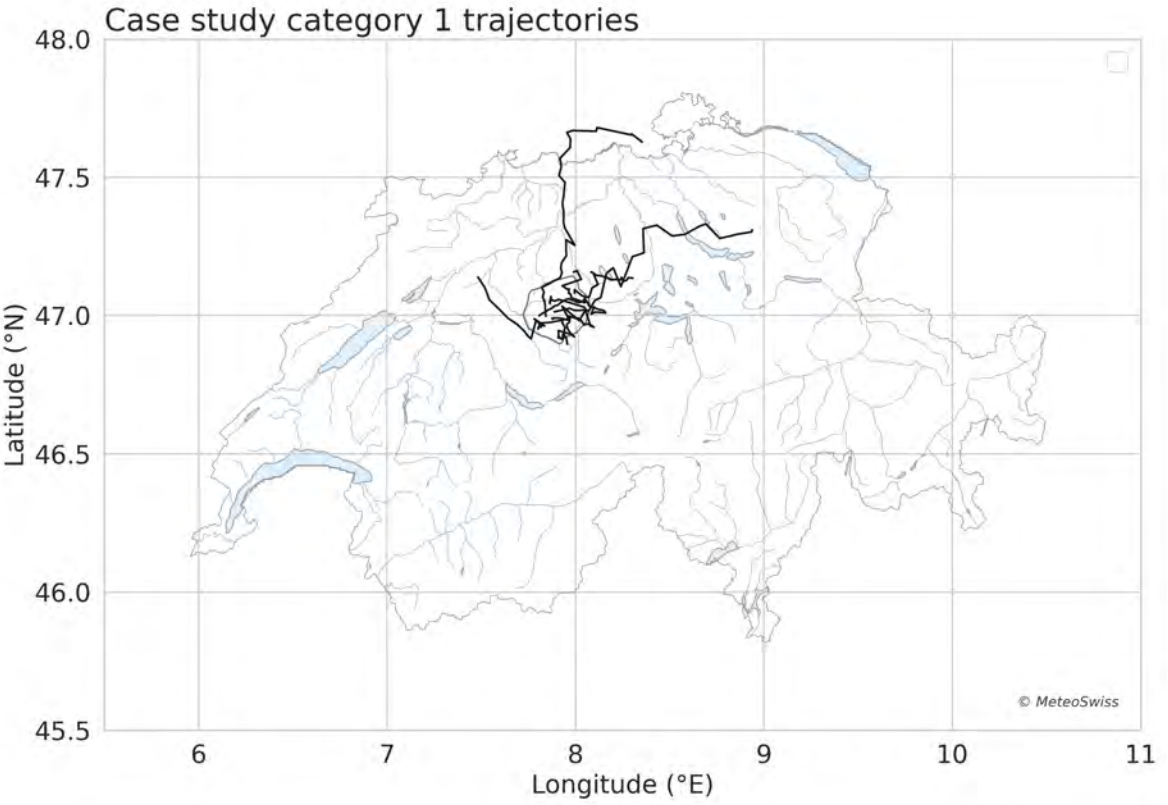

(a) Trajectories of the 11 category 1 hail cells.

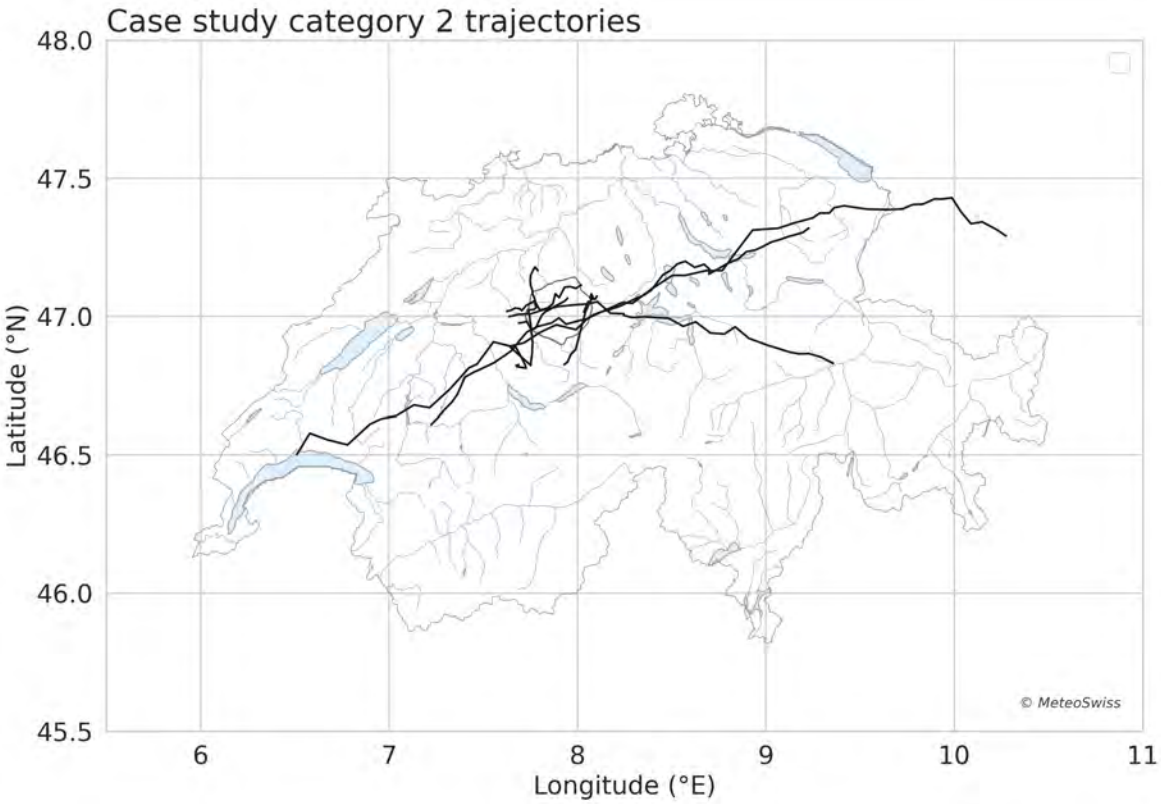

(b) Trajectories of the 7 category 2 hail cells.

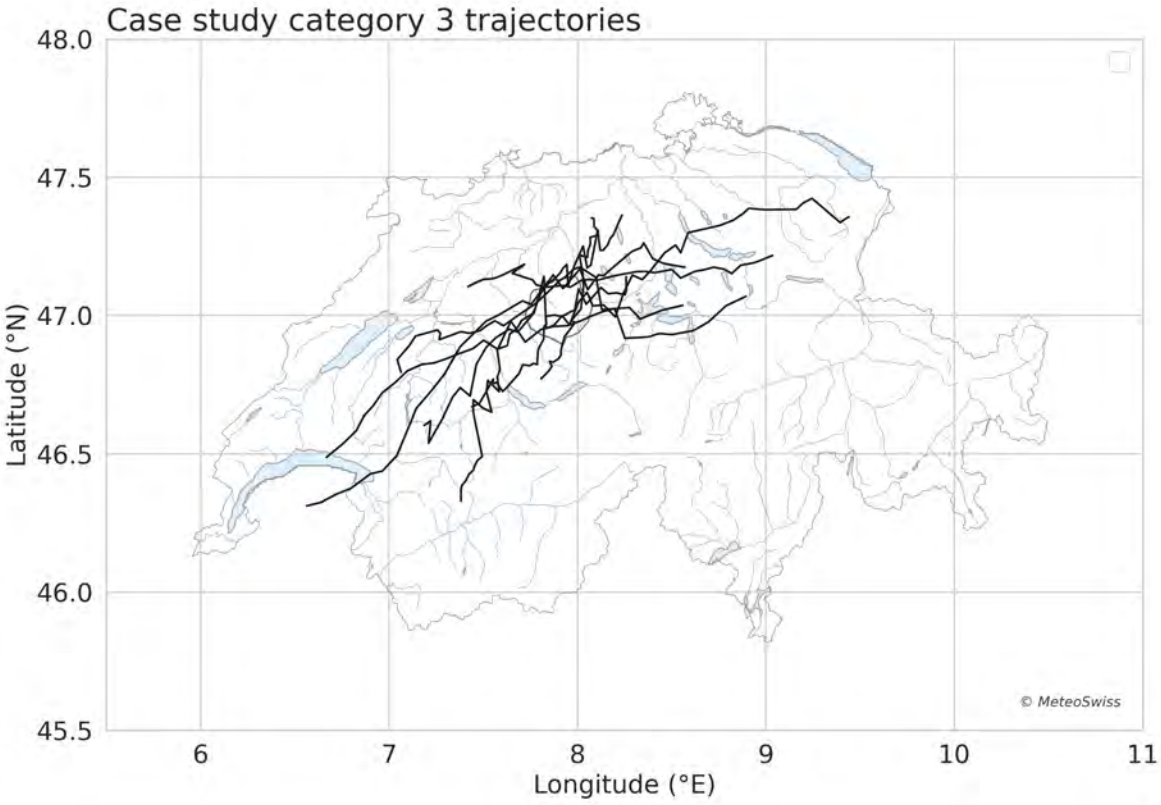

(c) Trajectories of the 8 category 3 hail cells.

Figure 8: Trajectories of all case studies.

3.6 Mann-Whitney-U Test

In this master thesis, many analyses are performed with three categories. The Mann-Whitney-U test is used to test if the three samples show significant differences.
The Mann-Whitney-U test, also called Wilcoxon-Mann-Whitney test or Wilcoxon-rank-sum test, is a non-parametric rank-sum test. It tests for the relative shift of two non-paired samples. The test statistic U is calculated by comparing the sums of ranks of the different groups (Equation 1).

$$U = n_1 n_2 + \frac{n_1(n_1 + 1)}{2} - R_1 \tag{1}$$

Where n_1 is the size of the sample with the larger sum of ranks and n_2 is the size of the sample with the smaller sum of ranks, respectively. R_1 is the larger of the sums of ranks. U can be standardized in a following step and compared to the standard normal distribution for significance testing. The assumptions are that the distributions differ in location only and that the sample values are independent (Mann and Whitney, 1947; Frei, 2020).

4 Results

4.1 Interview

The goal of the interview was to learn about the specific weather dynamics that play a role in triggering a hailstorm in the Napf region. Three processes were pointed out that could be possible reasons or mechanisms why the Napf hot spot exists. Henceforth, these are the hypotheses that are analysed and tested in this master thesis to answer the research questions asked in chapter 1:

- *[1] In the Emme valley, oftentimes a low-level boundary layer channel flow from the north-west or north-north-west is observed. At the same time, the wind direction just above the boundary layer is during the daytime often west-south-west. This configuration leads to an increased vertical wind shear forced by the Emme valley. In the Aare valley just next to the Emme valley, the exact same flow configuration is observed, too.*

- *[2] The Napf is sometimes called 'Inselberg', which means 'island mountain'. Only in the south on the Napf there are mountains - in the North, the East and the West the terrain is relatively flat. Therefore, one can roughly say that lower-lying areas lie to three sides of the Napf region, whereas in regions along the pre-Alps without such topography, this is the case only for two. As a consequence, it can be expected that relatively more moisture from the boundary layer is available to storms around the Napf region than in other pre-Alpine areas.*

- *[3] Thermo-topographic wind systems are on all sides of the Napf as well as "Talwinde", which all meet at the summit of the Napf and lead to convergence.*

4.2 Relative Frequency Analysis

The results of the comparison of the frequency of hailstorms compared to all thunderstorms is summarized in table 8. In the Napf region the relative frequency is with 5% twice as high than in the Albis region with 2.5%, or the whole area of Switzerland with 2.4%. The analysis was performed separately for the years 2002-2012 and 2013-2020, because in 2013 the new radar generation was established. No significant differences were found.

	Absolute # of hailstorms	**Absolute # of thunderstorms**	**relative frequency of hailstorms**
Napf	515	10'462	5%
Albis	539	21'852	2.5%
CH	32'714	1'536'080	2.4%

Table 8: Relative frequency of hailstorms compared to thunderstorms, including data from 2002-2020.

4.3 Diurnal Cycle

Figure 9 shows the diurnal cycle of the first detection time of the hail cells. This analysis was performed to compare the diurnal cycle of the three categories. The distribution shows that there is a strong dial cycle for all of the categories. It looks similar for all three categories. Few hailstorms form during the early morning hours. The number of hail cells start increasing at 10 am UTC, reach an afternoon peak and decrease in the evening. There is a late night accumulation of first detections of hail cells shown for category 3 from 9 to 10 pm. However differences in the diurnal cycle need to be interpreted carefully, because the data set is rather small.

4.4 Annual Cycle

Figure 10 shows the annual cycle of the 279 Napf hailstorms sorted by their category. This analysis was performed in order to find out if the hail cells occur distributed over

the whole hail season, which extends from April to September. April 1st lies in week 13, September 30th, the end of the hail season, is in week 39. In total 15 hail cells developed in April. 15 hail cells is 5.4% of the total 279 hail cells. In September, 6 hail cells developed. 6 hail cells are 2.2% of the total 279 hail cells. By reducing the hailstorm data set from 279 to 258, the ERA5 data is narrowed down from 6 to 4 months. The data becomes more robust and the yearly cycle becomes clearer by eliminating the first and the last month of the hail season, namely April and September. Therefore, all further data analyses are performed with 258 hail cells.

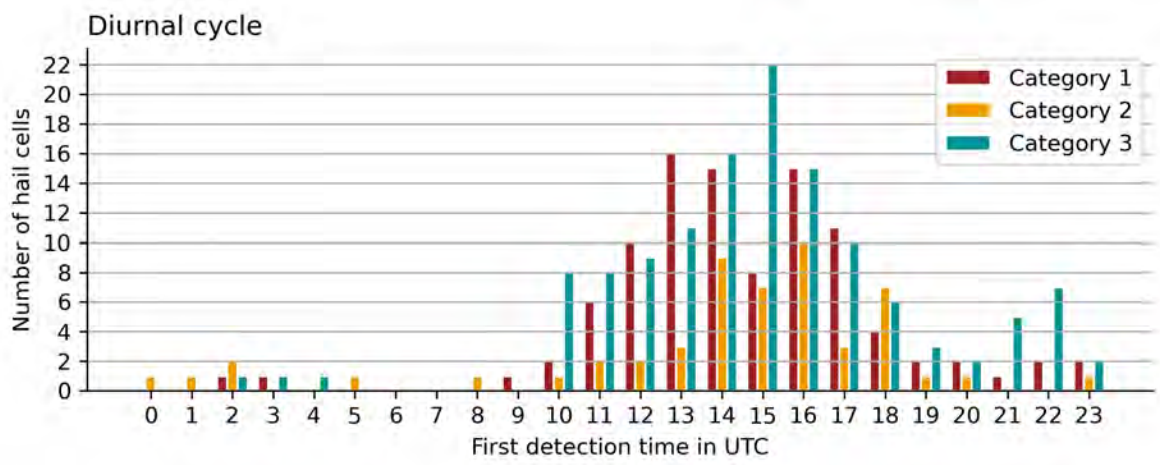

Figure 9: Diurnal cycle of the 279 Napf hail cells from 2002-2020.

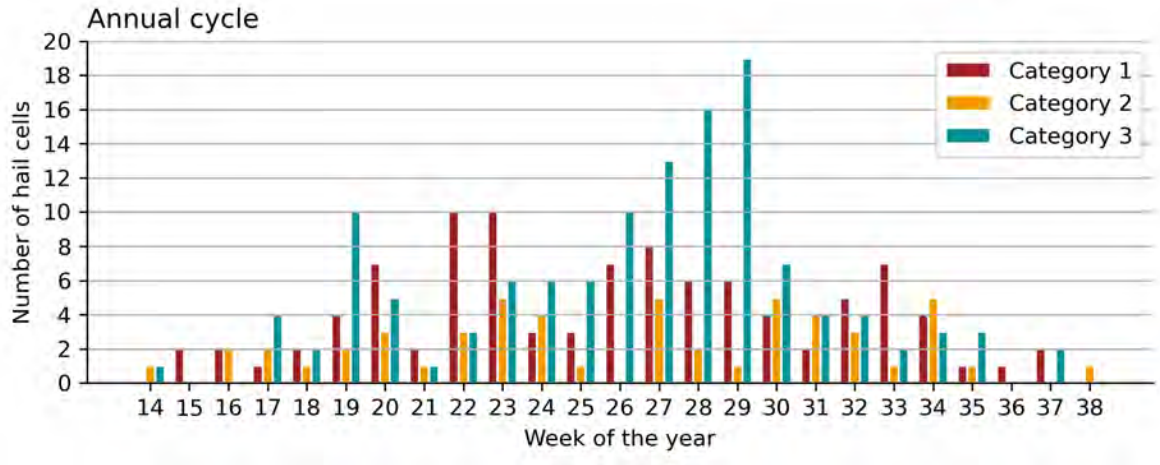

Figure 10: Annual cycle of the 279 Napf hail cells from 2002-2020.

4.5 Category Analyses

Storm Characteristics

The category analysis was performed in order to compare the storm characteristics of the three categories, see table 9. The locally triggered storms, category 1, have the shortest median path length with 30 km. The imported cells of category 3 show a median path length of 102 km. The median path length of category 2 storms lies with 63 km inbetween category 1 and 3. The category 1 median path length is significantly shorter on the 5% level than the category 2 median path length, and the category 2 median path length is significantly shorter than the category 3 median path length on the 5% level.

The median area of the convective cells is largest for category 3 hail cells with 404 km^2. For category 2 hailstorms the median area of the convective cells is 248 km^2, and 208 km^2 for category 1 hail cells. The median area of the convective cells of the category 1 hail cells is not significantly shorter than the median area of the convective cells of the category 2 hail cells on the 5% level. However, the median area of the convective cells of the category 2 hail cells is significantly shorter on the 5% level than the median area of the convective cells of the category 3 hail cells.

The median lifetime is shortest for category 1 cells with 85 min. Category 3 cells have with a median of 145 min the longest duration. The lifetime of category 2 storms lies with 100 min on median in between category 1 and 3. The median lifetime of category 1 hail cells is significantly smaller on the 5% level than the median lifetime of category 2 hail cells. The category 2 hail cells have a significantly lower median life time than the category 3 hail cells on the 5% level.

The median maximal MESHS is smallest for the category 2 cells with 27 mm. Category 1 has a median maximal MESHS of 33 mm. The largest median maximal MESHS is found in category 3 with 50 mm. The median maximal MESHS of category 2 hail cells is significantly smaller on the 5% level than for category 1. The median maximal MESHS of the category 2 hail cells is significantly smaller than the median maximal MESHS of the category 3 hailstorms on the 5% level.

The results of the Mann-Whitney-U tests can be found in the appendix.

	Category 1	**Category 2**	**Category 3**
Path length [km]	30 (45)	63 (71)	102 (103)
Area of the convective cells [km^2]	208 (204)	248 (174)	404 (224)
Lifetime [min]	85 (73)	100 (80)	145 (103)
MESHS max [mm]	33 (20)	27 (16)	50 (20)

Table 9: Median of the storm characteristics path length, area of the convective cells, lifetime and maximal MESHS for the three clusters. In brackets the interquartile range (IQR).

Weather Types

The most frequent weather types to produce hailstorms are south-west, high pressure distributions and flat pressure distributions (Table 10). 32% of the category 3 hail days occur during the south-west weather type, and 32% during a high pressure distribution. A flat pressure distribution occurred for 24% of the category 3 hail days. The remaining 12% of the category 3 hail days were during a west weather type, a south weather type, or a low pressure distribution. 36% of the category 2 hail days were during a south-west weather type. 31% of the category 2 hail days occurred at the time of a flat pressure distribution and 20% during a high pressure distribution. The remaining 13% of the category 2 hail days were during a west weather type, a south weather type, or a low pressure distribution. 48% of the category 1 hail days were during a flat pressure distribution and 24% at the time of a high pressure distribution. A total of 72% of the category 1 hail days occurred during 500 hPa wind speeds below 7 m/s, per definition. 19% of the category 1 hail days occurred during a south-west weather type. The remaining 9% of the category 1 hail days were during a west weather type, or a south weather type.

	W	**SW**	**NW**	**N**	**NE**	**E**	**SE**	**S**	**low pd**	**high pd**	**flat pd**
Category 1	5	19	0	0	0	0	0	4	0	24	48
Category 2	9	36	0	0	0	0	0	2	2	20	31
Category 3	7	32	0	0	0	0	0	2	3	32	24

Table 10: Prevailing weather types during the hail days in percentage [%]

ERA5 Box Plots

Category 1 to 3 include all days on which hailstorms crossed the Napf region. Category 4 and 5 are the reference categories introduced in section 3.4. Figure 11 (a) shows the distribution of the convective available potential energy CAPE. The median CAPE value of category 1 is 792 J/kg, 1061 J/kg for category 2 and 1027 J/kg for category 3. The CAPE of category 1 is significantly smaller than the CAPE of categories 2 and 3 on the 5% level. All p-values and test statistics of the significance tests can be found in the appendix. Reference category 4 including non-hail days shows a median CAPE of 43 J/kg and reference category 5 shows a median CAPE of 626 J/kg.

Figure 11 (b) shows the convective inhibition CIN. The median CIN for category 1 is 188 J/kg, for category 2 255 J/kg and 247 J/kg for category 3. There are no significant differences between the first three categories. The median CIN of category 4 is 51 J/kg and for category 5 187 J/kg. According to ECMWF (2021), CIN values greather than 200 J/kg are considered high. In a publication of Davies (2004), CIN is considered "relatively large" with values of 50 - 150 J/kg. A big part of the CIN values are passing the 200 J/kg threshold set by ECMWF (2021). Therefore, the CIN values overall are considered very uncertain. The reason for the extremely high ERA5 CIN values could not be detected.

Figure 11 (c) shows the 2 metre temperature. The median 2 metre temperature for category 1 is 24.0 °C, 24.9 °C for category 2, and 24.4 °C for category 3. There are no significant differences between the first three categories. Category 4 has a median 2 metre temperature of 19.6 °C, and category 5 of 22.6 °C.

Figure 11 (d) shows the wind speed at 500 hPa. For category 1 the median wind speed is 8.2 m/s, 13.9 m/s for category 2, and 14.1 m/s for category 3. On days where locally triggered cells (category 1) occur, the wind speed is significantly lower on a 5% level than for days on which imported cells (category 2 and 3) were observed. 12.4 m/s is the median wind speed for category 4 and 12.8 m/s for category 5.

Figure 11 (e) shows the wind speed at 850 hPa. The 850 hPa wind speed for category 1 is 2.6 m/s, 3.6 m/s for category 2, and 2.9 m/s for category 3. Category 1 days show significantly lower wind speeds at 850 hPa than category 2 days with a confidence level of 95%. The difference of the category 1 and category 3 days is not significant on the

5% level.

Figure 11 (f) shows the bulk wind shear between 500 and 850 hPa. The bulk wind shear is 7.9 m/s for category 1, 10.7 m/s for category 2 and 10.7 m/s for category 3. Category 1 days show a significantly lower bulk wind shear on the 5% level than category 2 to 5.

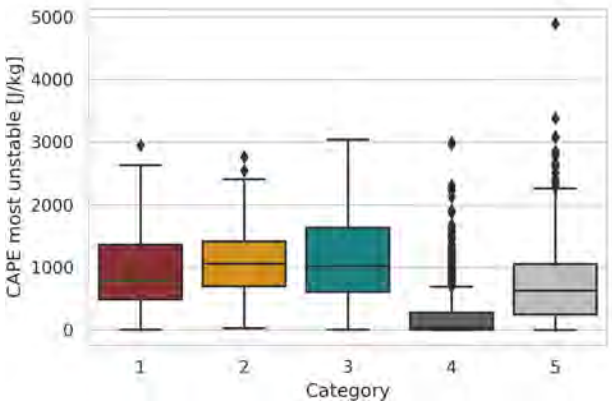

(a) CAPE most unstable

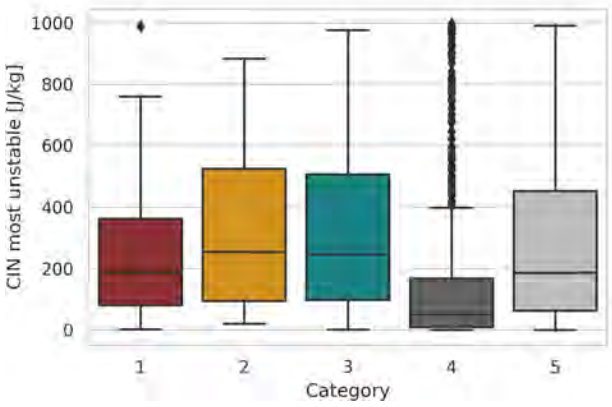

(b) CIN most unstable

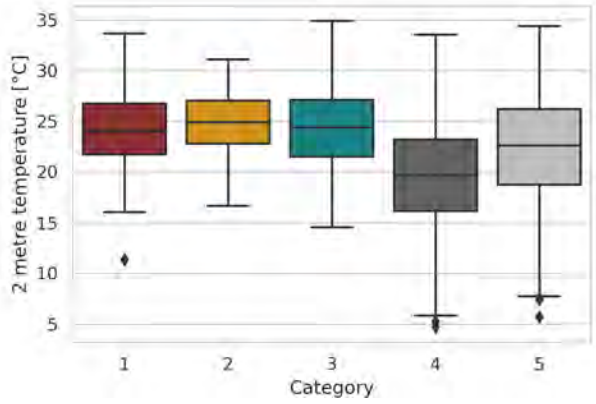

(c) 2 m temperature

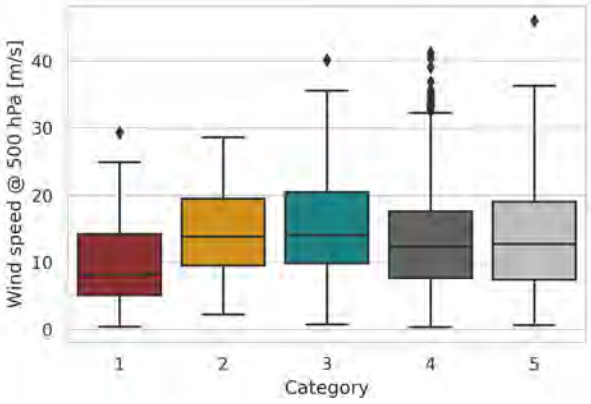

(d) Wind speed @ 500 hPa

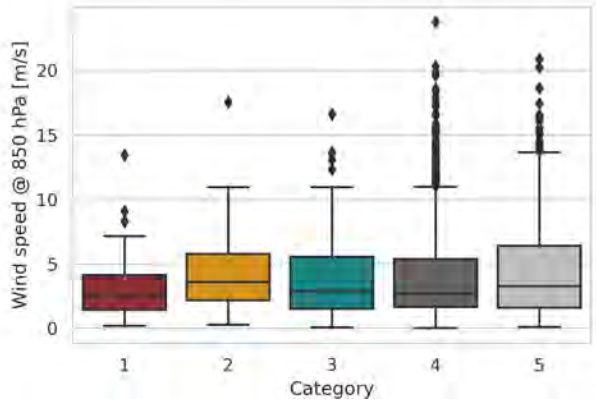

(e) Wind speed @ 850 hPa

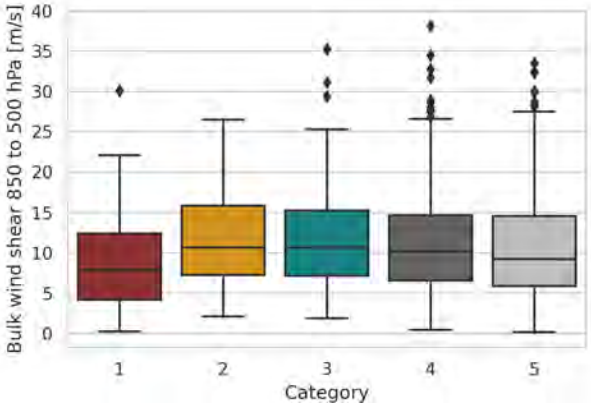

(f) Bulk wind shear 850-500 hPa

Figure 11: ERA5 boxplot analyses. The box of each boxplot includes the middle 50% of the data. The lower end of the box corresponds to the first quartile (Q1), the line in the middle of the boxplot to the second quartile (Q2), and the upper end of the box to the third quartile (Q3), respectively. The whiskers have a maximal length of 1.5*IQR, while the IQR is the interquartile range, Q3-Q1.

ERA5 Composite Maps

Composite maps give a spatial overview of the meso-scale weather pattern during hail days in the Napf region.

Figure 12 shows the median vertical wind shear for category 1 days. The vertical wind shear reaches lowest values on the north eastern edge of the domain, in Germany, with values of 2 m/s. Highest values are reached in France, next to the border to Italy with values up to 9 m/s. The 500 hPa geopotential height is at 5750 meters over central France. Over Switzerland it is at 5775 metres and over Italy it is at 5800 metres. The gradient in geopotential height is low. The contours are aligned from Southwest to Northeast. This implies an upper-level wind direction from the Southwest with low wind speeds which is in agreement with the results of the weather type analysis.

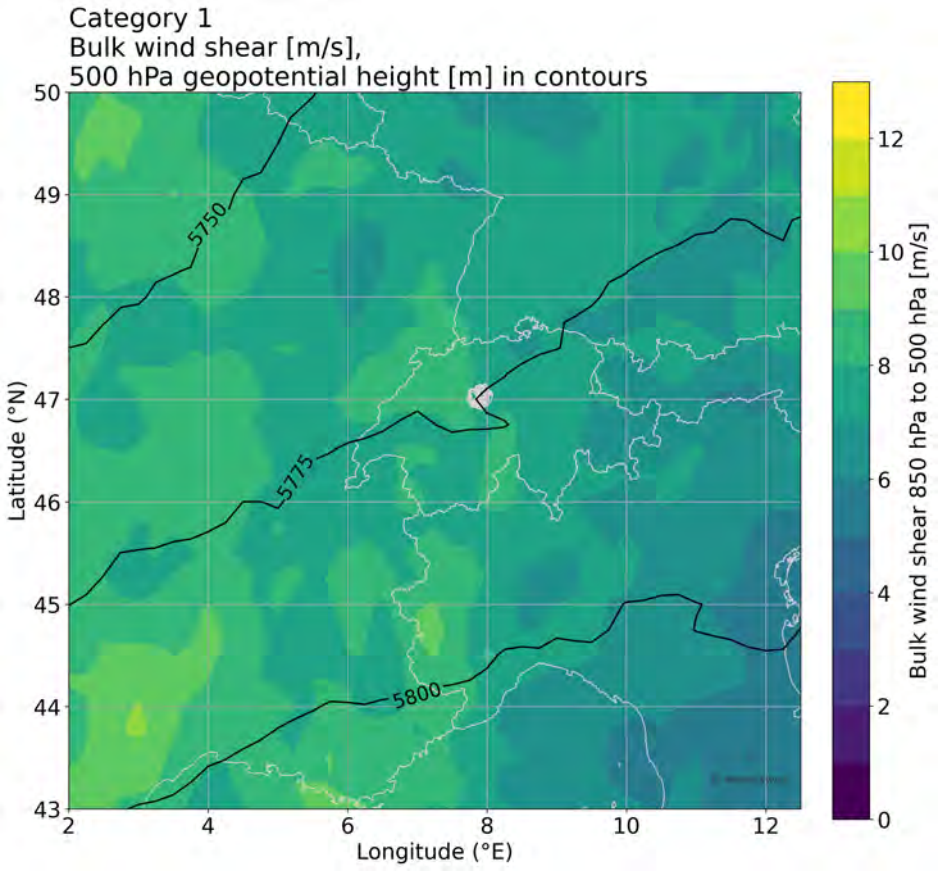

Figure 12: Bulk wind shear (shaded) and geopotential height at 500 hPa (contours), 12 UTC median of all category 1 hail days for April to August 2002-2020. The light grey lines show the country borders and the demarcation of the Napf region. The light grey dots filling the Napf region are the first detection locations of all category 1 hail cells.

Figure 13 shows the median vertical wind shear for category 2 days. Lowest wind shear, with values of 4 m/s can be observed over Italy, on the east coast, as well as on the west coast of the Mediterranean. Highest vertical wind shear with values exceeding 11 m/s are reached in France at a latitude of about 46°N and 3°E, in the French Alps at the border to Italy and in the Swiss Alps south of the Napf region. The 500 hPa geopotential height is at 5725 metres over central France. Over the Jura Mountains, the 500 hPa geopotential height is at 5775 metres and at 43°N it is at 5825 metres. The contours show a Southwest to Northeast direction, with a gradient much higher than for category 1. This implies a dominant upper-level wind direction from the Southwest with stronger wind speeds than for category 1. This result is in agreement with the results of the weather type analysis.

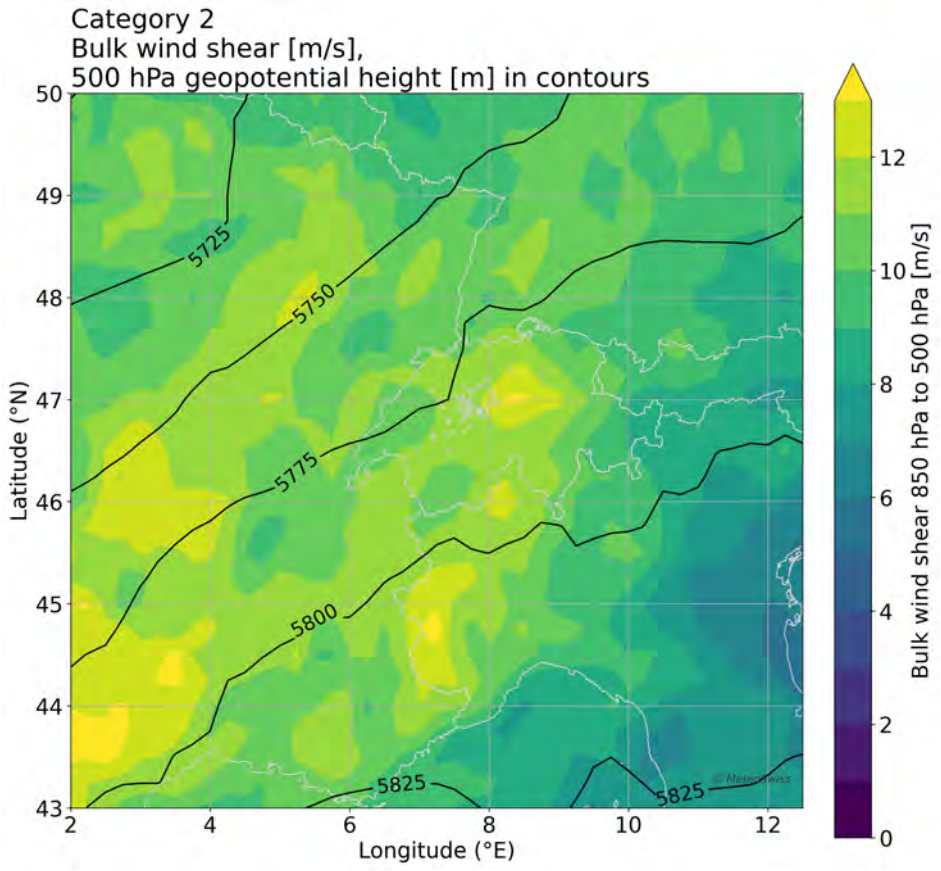

Figure 13: Bulk wind shear (shaded) and geopotential height at 500 hPa (contours), 12 UTC median of all category 2 hail days for April to August 2002-2020. The light grey lines show the country borders and the demarcation of the Napf region. The light grey dots are the first detection locations of all category 2 hail cells.

Figure 14 shows the median vertical wind shear for category 3 days. Lowest wind shear occurred to the west of the French Alps, as well as over Italy at 43.5°N with values of 5 m/s. Highest wind shear was reached all along the French Alps with values exceeding 11 m/s. The 500 hPa geopotential height is at 5725 metres over France in the north-western edge of the domain. In the French Jura Mountains it is at 5775 metres and over the Mediterranean the geopotential height at 500 hPa is at 5825 metres. The contours show a Southwest to Northeast direction, with a gradient much higher than for category 1. The dominant upper-level wind direction is from southwest with stronger wind speeds than for category 1. This result is in agreement with the results of the weather type analysis.

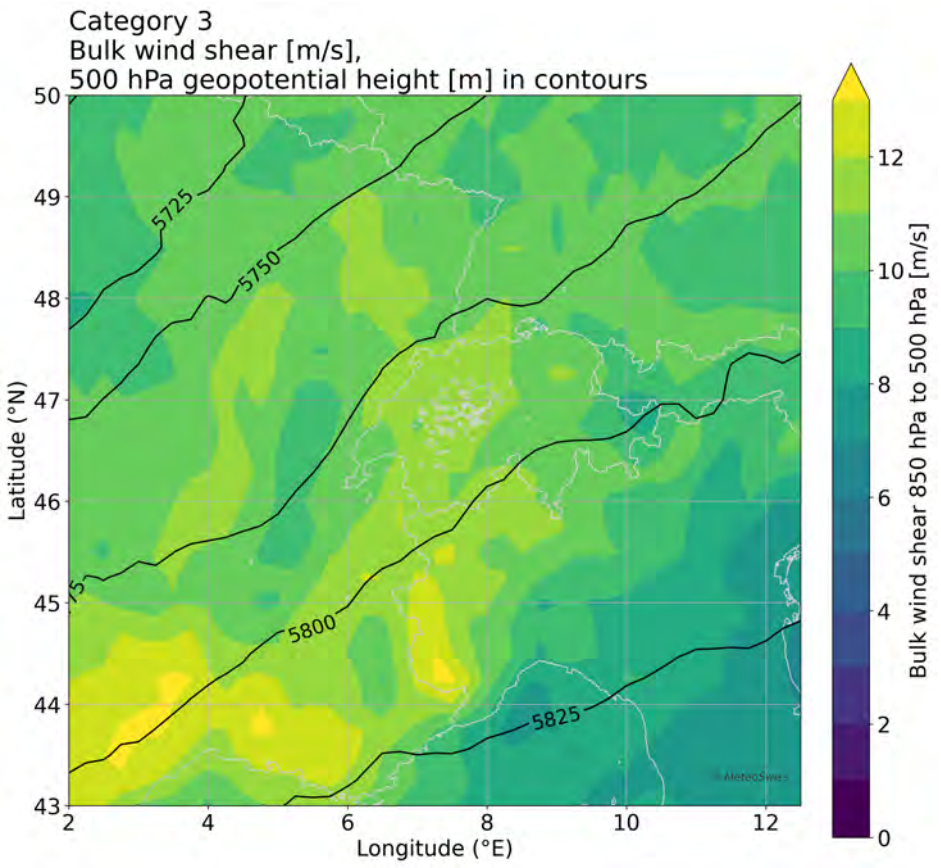

Figure 14: Bulk wind shear (shaded) and geopotential height at 500 hPa (contours), 12 UTC median of all category 3 hail days for April to August 2002-2020. The light grey lines show the country borders and the demarcation of the Napf region. The light grey dots are the first detection locations of all category 3 hail cells.

4.6 Case Studies

In the case studies, the high resolution COSMO data is used. Due to the hourly temporal and the 1km spatial resolution, local phenomena, as described in the hypotheses in section 4.1, can be analyzed. Each case study describes only one time step, namely 1 hour before the hailstorm of interest developed.

To investigate the first hypothesis, the bulk wind shear is used. The first hypothesis states that there is wind shear due a low-level channel flow in the Aare- and Emmental from north-west and a wind direction just above the boundary layer of west-south-west (see chapter 4.1).
The left column of figure 15 contains the category 1 case studies, the center column the category 2 case studies and the right column the category 3 case studies. On figure 15 category 1 hailstorms show overall lower bulk wind shear with values of around 6 m/s. There is only one day (Figure 15 (b) 2018-05-31), on which two category 1 storms occurred, with a bulk wind shear exceeding 18 m/s.

Next, three case studies will be presented. Each of the case studies is representative of one category in terms of bulk wind shear.
The first case study, figure 16, is a case study of a category 1 hailstorm. Figure 16 shows the bulk wind shear on July 6th 2016 at 11:00 UTC. One hour later, a category 1 hailstorm developed (pink dot). The pink line shows the trajectory of the hailstorm. The grey lines show all the other hailstorms that developed on July 6th in 2016. The bulk wind shear is below 6 m/s in the northern pre-Alps and in the largest parts of the Swiss plateau. Near Basel and in the Jura Mountains some regions reach a bulk wind shear of over 14 m/s. The grey lines show that many other hailstorms with short track length initiated that day under these conditions. Hence, the conditions on that day were suitable for the formation of short-tracked hail cells.
The second case study, figure 17, is a case study of a category 2 hailstorm. Figure 17 shows the bulk wind shear on May 30th 2018 at 12 UTC. The bulk wind shear is approximately 15 m/s in the Napf region. To the Southwest of the Napf region, where the

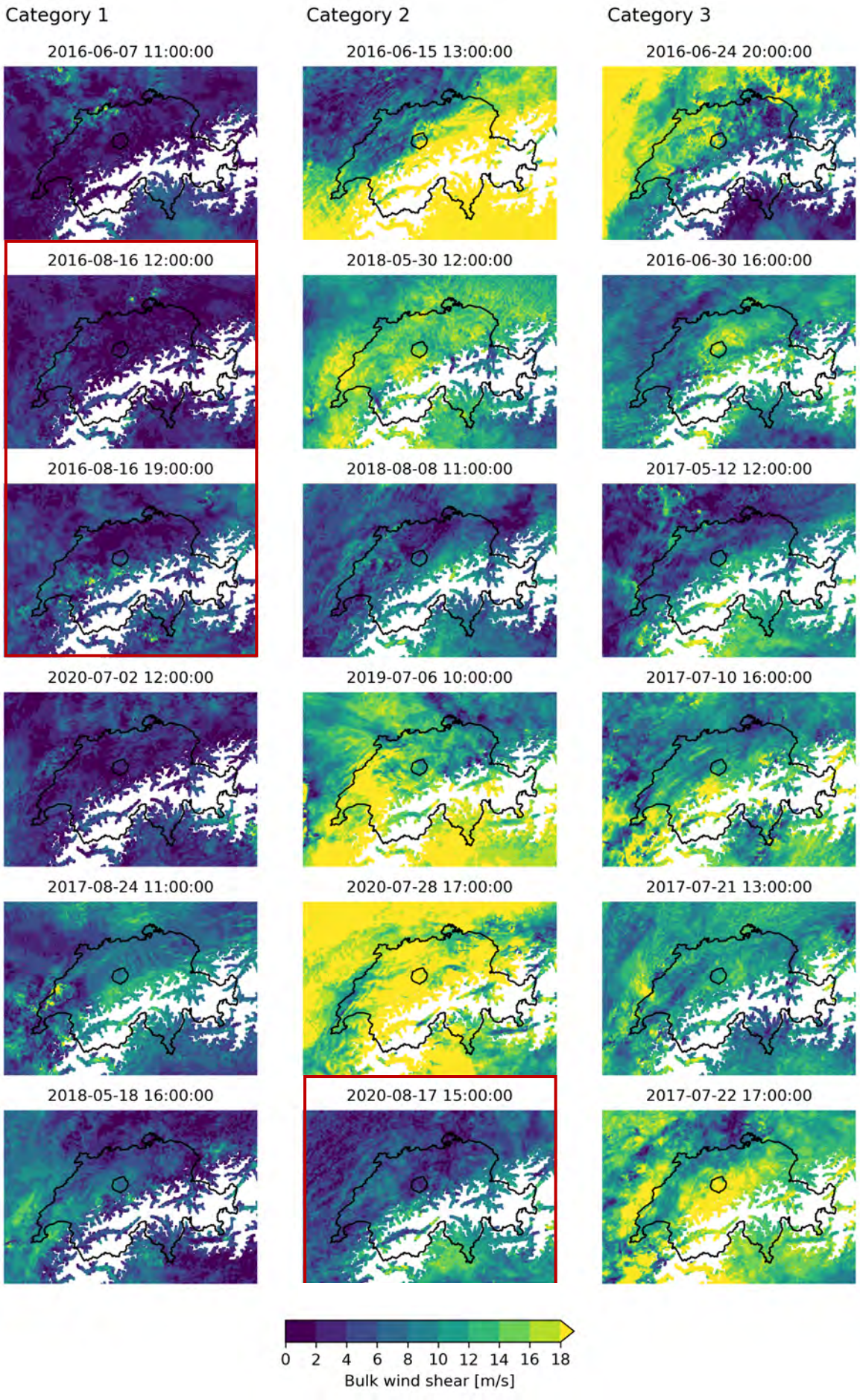

(a) Bulk wind shear for case study 1-6 of each category.

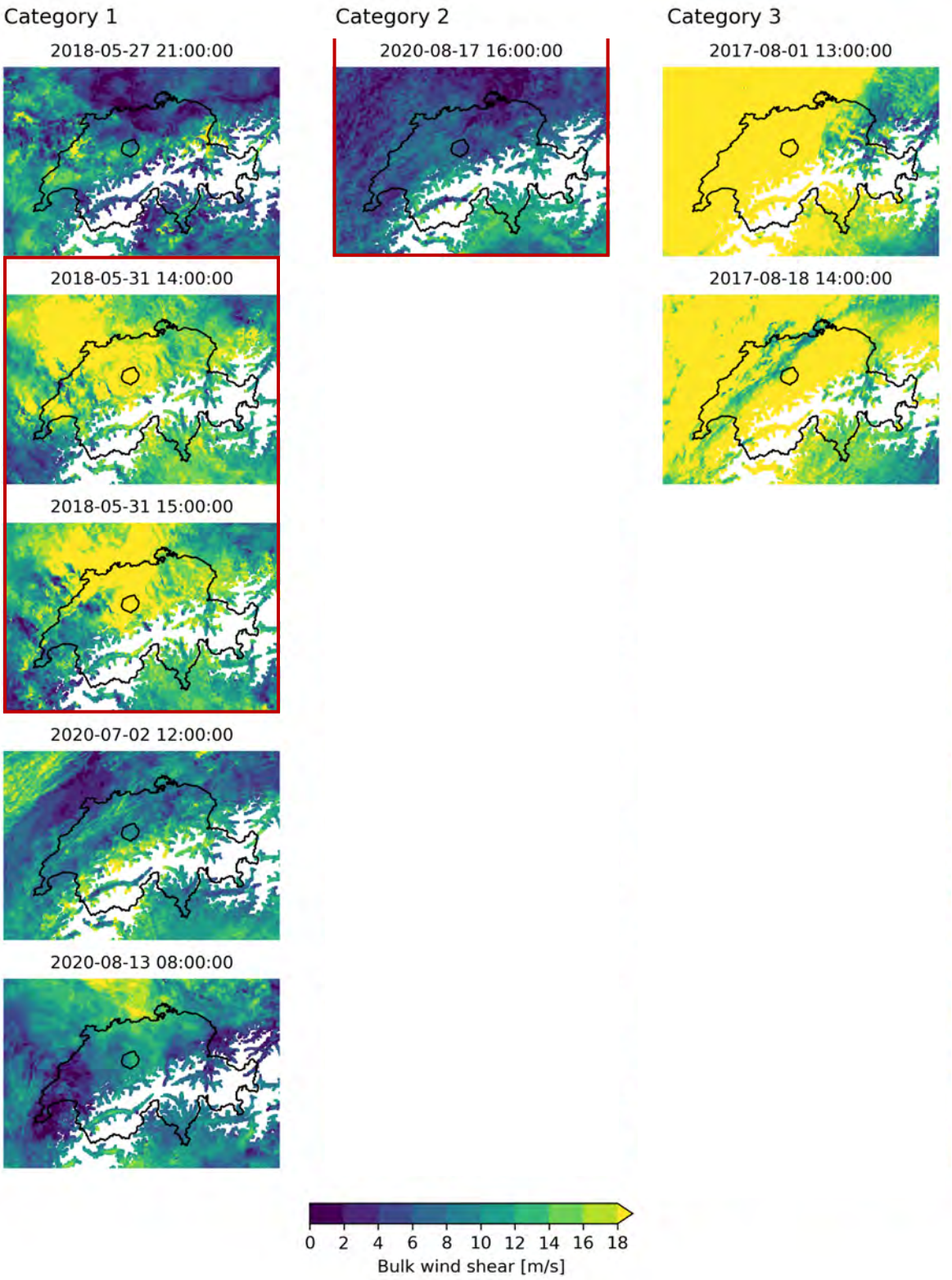

(b) Bulk wind shear for case study 7-11 of each category.

Figure 15: Bulk wind shear 850 to 500 hPa for all case study hailstorms. Time in UTC, one hour before the respective case study hailstorm was first detected. The red outline connects case studies occurring on the same day.

Napf hail cell was first detected (pink dot), values of over 18 m/s are reached. Other hailstorms that initiated that day, depicted in grey lines, show approximately the same path length as the Napf hail cell. Hence, the conditions seem to have been suitable for rather short hail cell tracks similar to the ones of category 2 (63km in median).

The third case study, figure 18, is a case study of a category 3 hailstorm. Figure 18 shows the bulk wind shear on July 22nd 2017 at 17 UTC. The bulk wind shear is exceeding 18 m/s in the Napf region and to the south, as well as to the east of it. Other hailstorms that initiated on that day (grey lines) show very long track lengths, similar to the category 3 hail cell (pink line). Hence, the conditions that day were suitable for the formation of hail cells with a long path length.

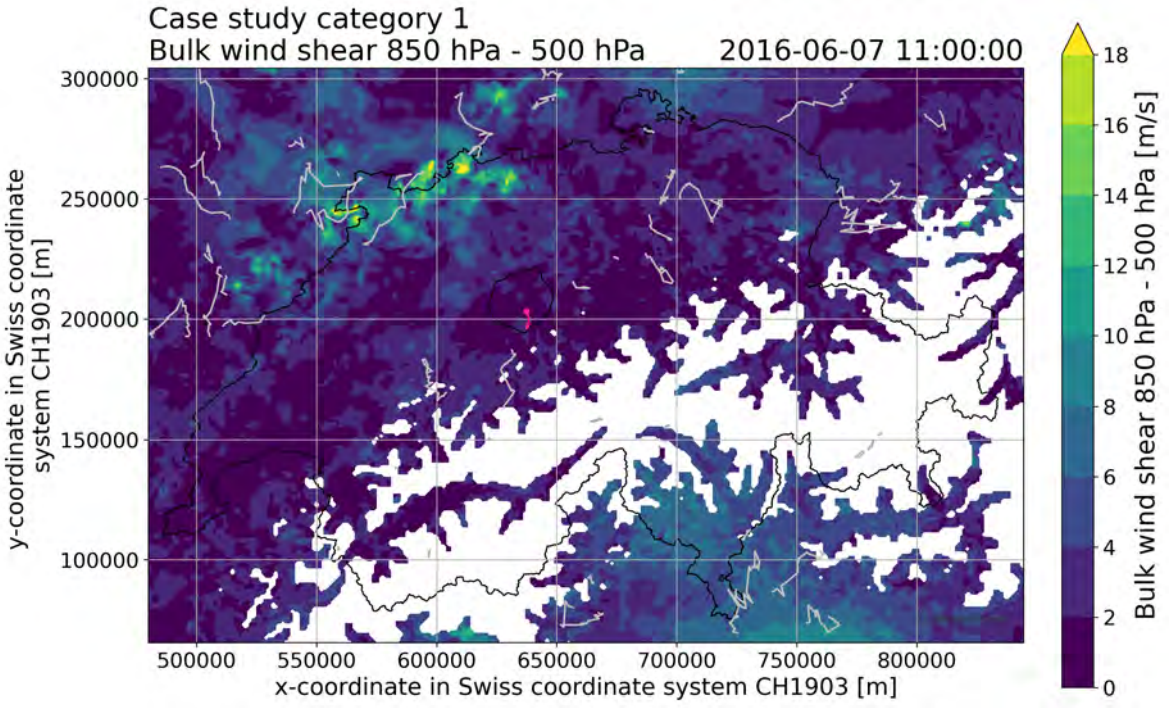

Figure 16: Bulk wind shear on 07.06.2016 11 UTC shaded, trajectory of one category 1 storm that developed at 12 UTC in pink, the genesis location is marked with a pink dot. All other trajectories of hailstorms on 07.06.2016 in grey, Napf region in black.

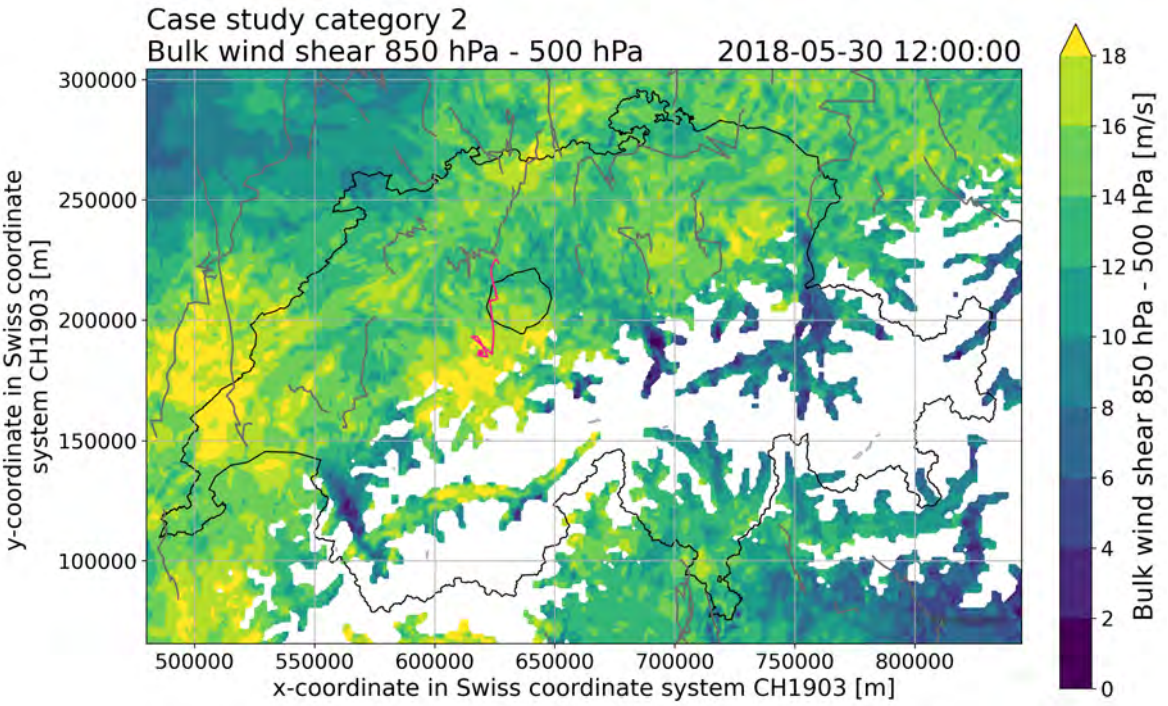

Figure 17: Bulk wind shear on 30.05.2018 12 UTC shaded, trajectory of one category 2 storm that developed at 13 UTC in pink, the genesis location is marked with a pink dot. All other trajectories of hailstorms on 30.05.2018 in grey, Napf region in black.

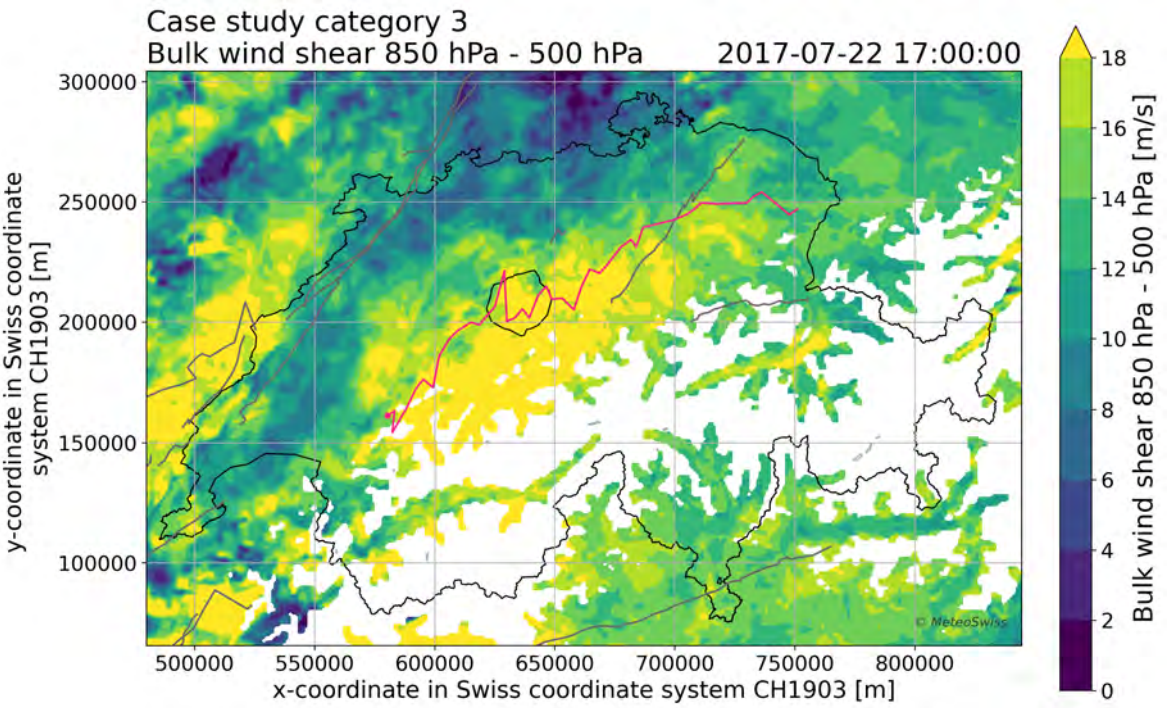

Figure 18: Bulk wind shear on 22.07.2017 17 UTC shaded, trajectory of one category 3 storm that developed at 18 UTC in pink, the genesis location is marked with a pink dot. All other trajectories of hailstorms on 22.07.2017 in grey, Napf region in black.

The second hypothesis states that the Napf is an 'island mountain' with flat terrain in the North, the East and the West. Therefore, the boundary layer is thick and more moisture is available for thunderstorms to develop than in topographies where no such island mountain situation is present (see chapter 4.1). In order to test this hypothesis, the Napf region moisture availability from the boundary layer would need to be evaluated against the moisture content of the lower atmosphere in a similar general setting of the northern Alpine pre-Alps without island-mountain topographies. In the scope of this thesis, only thunderstorm data for the primary study region were analysed and therefore, the hypothesis cannot be formally tested at this point.
However, as the moisture availability is still an important factor to understand the generation of severe thunderstorms, the boundary layer height at the time of first cell detection is analysed for the case study days of this thesis. Figure 19 shows the boundary layer height for all case study hailstorms. The boundary layer height varies for all categories between <300 m and >1800 m. The smallest value of below 300 m occurred in the evening or morning hours. Visually it is not possible to determine if any of the hailstorms were favoured due to a high boundary layer height. From the visual analysis, there are no obvious patterns that allow to differentiate between the case study days of the three categories.

The moisture availability was also analyzed by looking at the dew point temperature at 2m, see appendix figure A.3. The figure can be read analogous to figure 15. For the dew point temperatures, visually it was not possible to determine if any of the hailstorms were triggered due to a high dew point temperature.

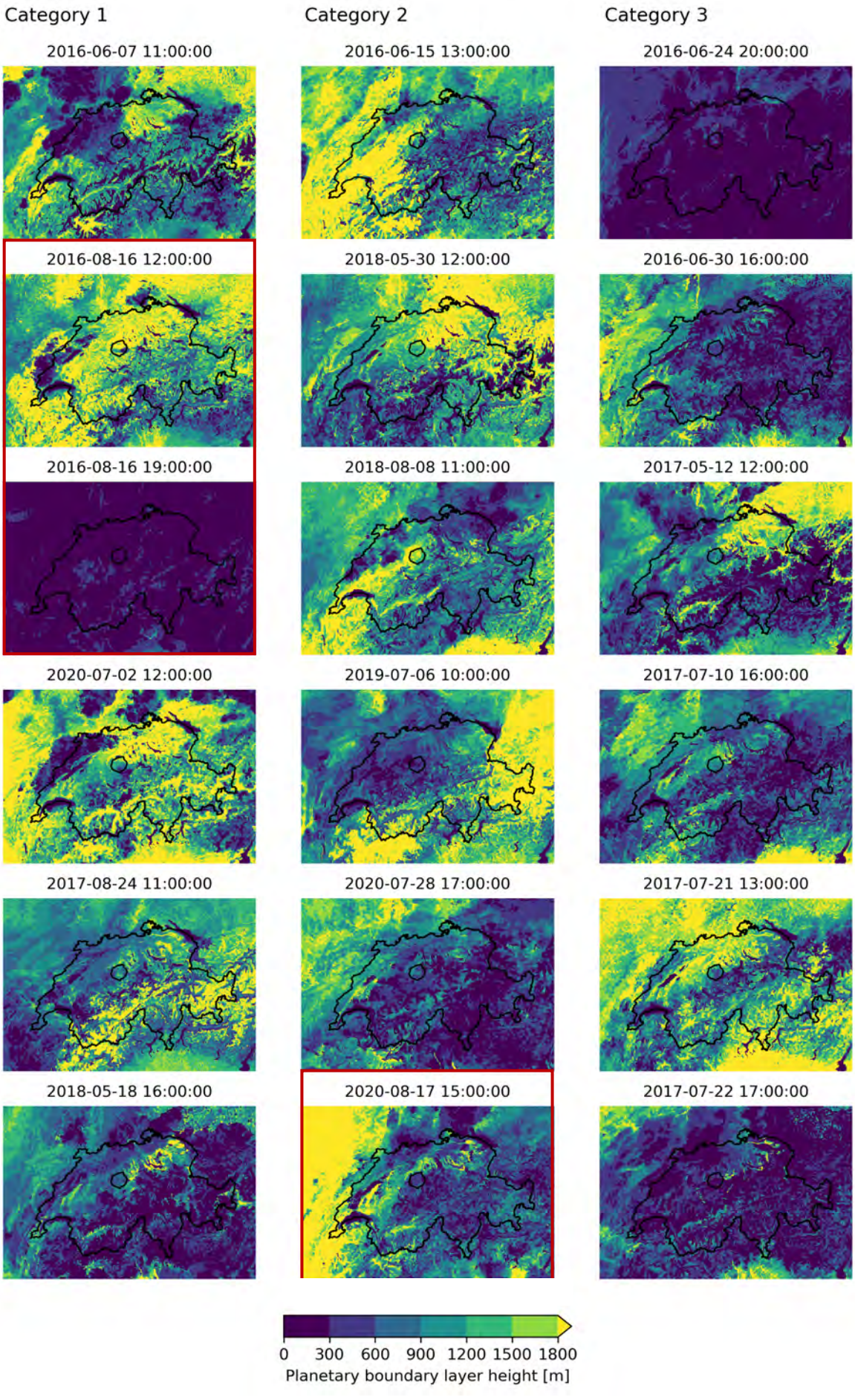

(a) Boundary layer height for case study 1-6 of each category.

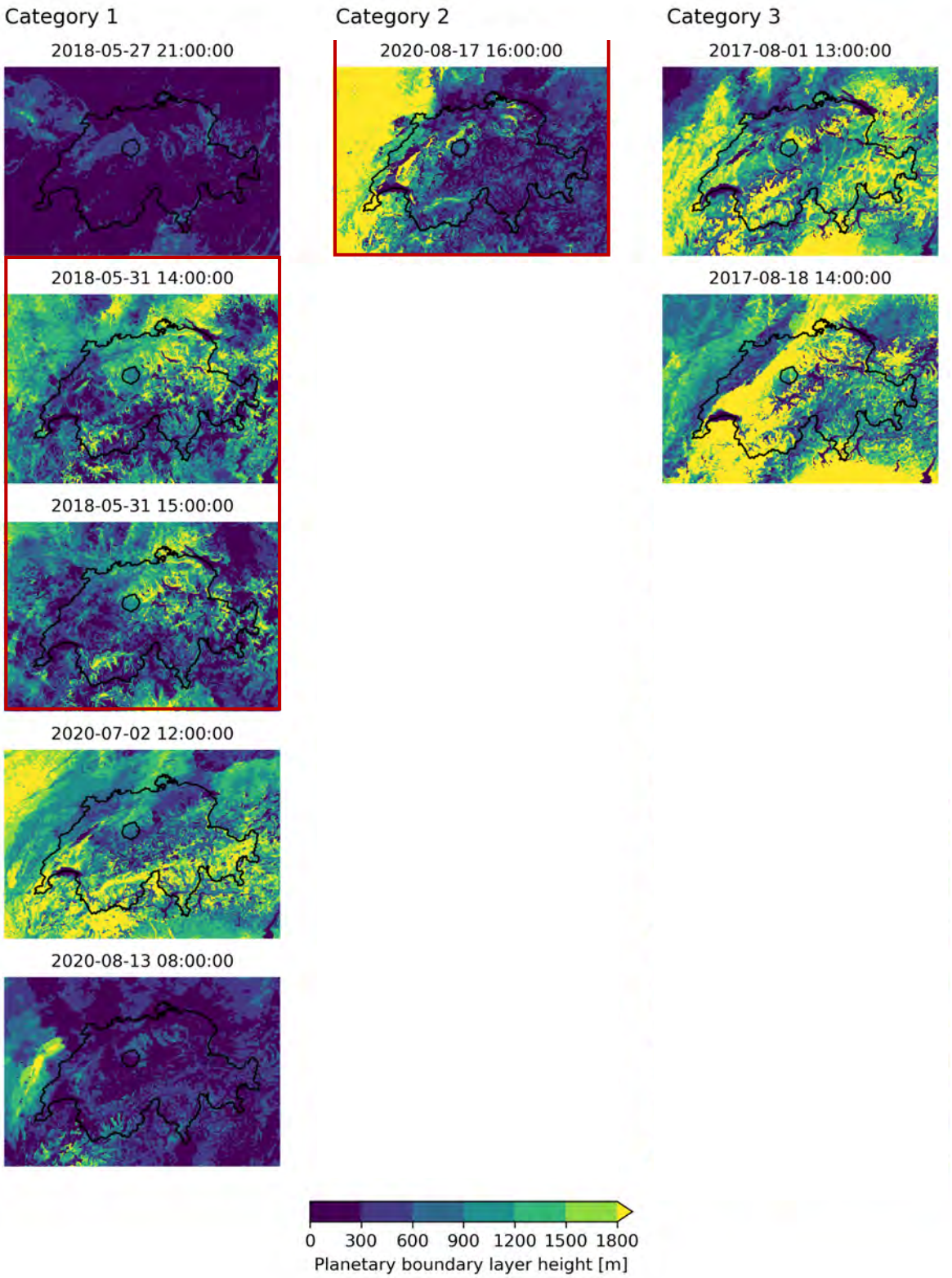

(b) Boundary layer height for case study 7-11 of each category.

Figure 19: Boundary layer height for all case study hailstorms. Time in UTC, one hour before the respective case study hailstorm was first detected. The red outline connects case studies occurring on the same day.

To investigate the first and the third hypotheses, wind fields are used. The first hypothesis states that there is wind shear due a low-level channel flow in the Aare- and Emmental from north-west, and a wind direction just above the boundary layer of west-south-west (see chapter 4.1). The third hypothesis states that there are valley winds that meet at the summits and lead to convergence (see chapter 4.1).
Figure 20 shows the wind vectors on May 31st 2018 at 15 UTC. One hour later, the hailstorm shown with the red trajectory developed. In Figure 20 the low-level boundary layer channel flow from the north-west can be detected in the Aare valley, marked by the orange square. The 500 hPa winds do not support the hypothesis. However, figure 20 shows that valley winds can be captured in the 850 hPa data. Thus, strong evidence that support the first hypothesis of the sheared environments should be found in this data. In all of the 23 case studies, no evidence supporting the hypothesis was found. Before rejecting this hypothesis, the 10m wind should be studied.
For the third hypothesis, the same argumentation holds true as mentioned above. As the 850 hPa data is able to capture valley winds, evidence for the third hypothesis should be found in this data. In none of the 23 case studies, evidence supporting the hypothesis was found. Before rejecting this hypothesis, the 10m wind should be studied.

In order to investigate the third hypothesis, divergence is used. The third hypothesis states that there are valley winds from all sides of the Napf that meet at the summit and lead to convergence (see chapter 4.1).
Negative divergence is equal to convergence and can therefore be used to detect convergence. Divergence is changing from negative to positive to negative values hourly (no figure). Thus, it was decided to renounce an interpretation of the divergence.

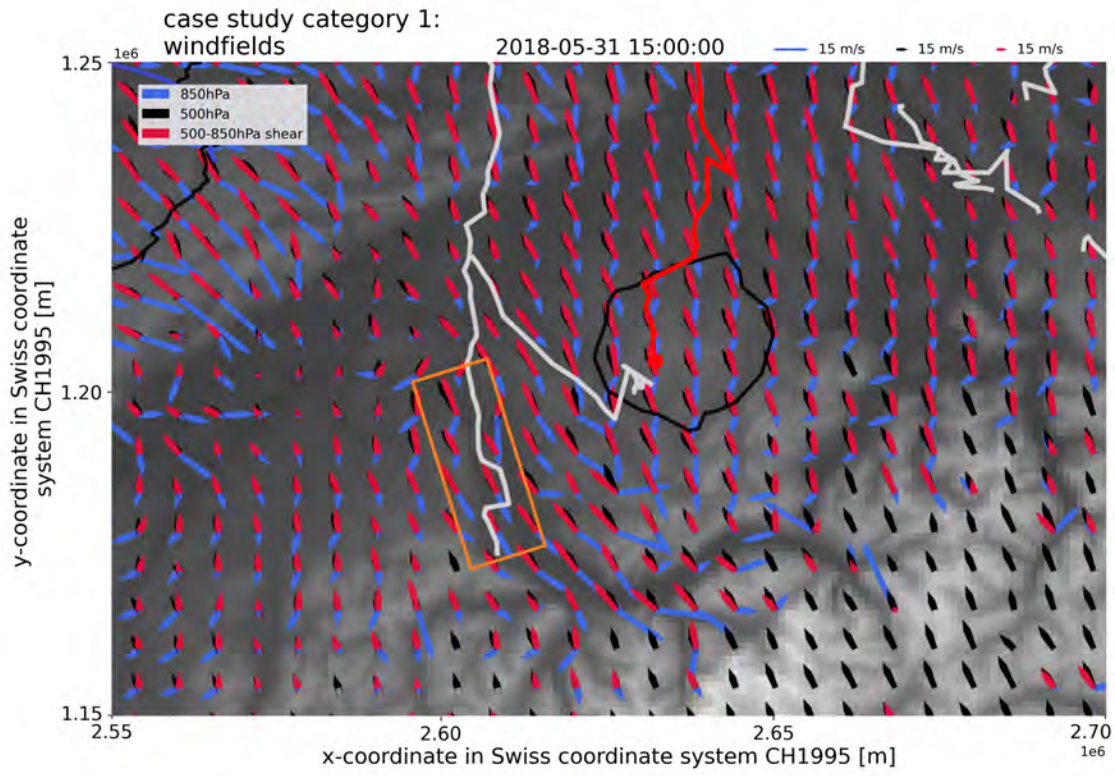

Figure 20: Wind vectors @ 500 (black) and 850 hPa (blue), and bulk wind shear (red) 500 to 850 hPa at 15 UTC on 31.05.2018. The grey shading in the background is the topography of Switzerland. The black circle depicts the Napf region and the orange square the Aare valley. The grey lines are all hailstorm tracks of the respective day and the red line is the storm track that crossed the Napf region and produced hail in the Napf region. The genesis location is marked by the red dot.

5 Discussion

5.1 Hypotheses

[1] In the Emme valley, oftentimes a low-level boundary layer channel flow from the north-west or north-north-west is observed. At the same time, the wind direction just above the boundary layer is during the daytime often west-south-west. This configuration leads to an increased vertical wind shear forced by the Emme valley. In the Aare valley just next to the Emme valley, in direction south-west, the exact same flow configuration is observed, too.

According to Doswell (1987), vertical wind shear is considered a crucial ingredient for hail development. The vertical wind shear influences the lifetime of storms, and it leads to the formation of multicell and super cell storms by separating the up and downdraft regions (Davies and Johns, 1993; Bluestein, 1993).

This first hypothesis was investigated by analyzing the bulk wind shear and the wind fields (section 4.6). The analysis of the bulk wind shear in figure 15 shows lower bulk wind shear over the of whole Switzerland for category 1 than for categories 2 or 3. From the bulk wind shear analysis in chapter 4.6, no increased vertical wind shear in the Emme or Aare valley can be detected. In a second analysis, the wind fields at 500 hPa, 850 hPa and the wind field of the bulk wind shear were examined. The findings are that in only 2 of the 23 case studies, the flow configuration described in the hypothesis was observed.

One important limitation of this analysis is the absence of the 10 metre wind. The 10 m wind variable does exist in COSMO, but it was not available in the data set used within this master thesis. It is not certain that the low-level boundary layer flow is captured in the 850 hPa wind that was used in the analysis. The 10 metre wind data would probably bring better results.

This hypothesis considers vertical wind shear in general. A separation of thermotopographic flow and forced channel flow in the low-level boundary layer could be made in further work.

[2] The Napf is sometimes called 'Inselberg', which means 'island mountain'. Only in the south on the Napf there are mountains - in the North, the East and the West the terrain is relatively flat. Therefore, one can roughly say that lower-lying areas lie to three sides of the Napf region, whereas in regions along the pre-Alps without such topography, this is the case only for two. As a consequence, it can be expected that relatively more moisture from the boundary layer is available to storms around the Napf region than in other pre-Alpine areas.

This second hypothesis was examined by analyzing the boundary layer height and the dew point temperature (figure 19 and A.3). However, since thunderstorm data were only analysed for the Napf region, no comparison of the available moisture could be done against other, otherwise similar areas. Further work could evaluate this thesis in more depth through comparing the total moisture availability against the hailstorm initiations for regions along the pre-Alpine areas of the northern Alps, considering for each region the topographic preconditions.
As moisture availability is one important factor to thunderstorm initiation, analyses of the boundary layer height and the 2m dew point temperature were carried out for the case study days of all categories. The main finding from this analysis is that neither in the boundary layer height analysis nor in the dew point temperature analysis obvious patterns that allow to differentiate between the case study days of the three categories were found.

[3] Thermo-topographic wind systems are on all sides of the Napf, as well as "Talwinde", which all meet at the summit of the Napf and lead to convergence.

This third hypothesis was analyzed by examining the wind fields at 850 hPa, and the divergence. The wind field analysis did not show any valley winds around the Napf. The analysis of the divergence did not provide any results due to the hourly

changing positive and negative values.
Here again, an important limitation for the wind field analysis is the absence of the 10 metre wind data. By using the 10 metre wind data, the valley winds could probably be captured. To assess the importance of valley winds and convergence in the Napf region, besides the 10 metre wind, station data from the MeteoSwiss station at the Napf could be used. Another approach to capture the convergence could be to look at the maximum daytime convergence together with the topography.

In the COSMO model, the hailstorms may have developed earlier or later than in reality, or not at all. It would therefore be important to make a statement about how transient or stationary the conditions were during the case studies. This could be done by analyzing each case study for 5 hours, starting two hours before the actual development of the hailstorm and ending two hours after it. Due to time reasons, this extensive analysis could not be realized within this master thesis.

5.2 Research Questions

[A] Why is the frequency of hail days higher in the Napf region? – Are the hail cells locally triggered or pre-existing and thus "imported" from other regions?

The categorisation in chapter 3.2 showed that 35% of the hail cells were locally triggered (category 1). 65% of the hail cells are category 2 or 3 hail cells, hence imported ones. As follows, locally triggered and imported hail cells both contribute a large fraction to the absolute number of hail cells in the Napf region. Thus, the situation in the Napf region is favorable for the triggering of local hail cells, but also hail cells that initiated in other regions do cross the Napf region. This fact is one explanation for the higher frequency of hail days in the Napf region than in other regions of Switzerland. The relative frequency of Napf hailstorms compared to Napf thunderstorms is with 5% twice as high as in the Albis region or in Switzerland overall. This finding serves also as an explanation for the higher frequency of hail days in the Napf region than in other

regions.

[B] What is the magnitude of the hailstorm characteristics of hail events that occur in the Napf region? Where the storm characteristics are path length, area, lifetime and max MESHS.

Generally, the path length, area, lifetime, and maximal MESHS increase from category 1 to category 2, and again from category 2 to category 3 (table 9). The maximal MESHS is in that case an exception. Smallest maximal MESHS values are observed for category 2 hailstorms with 27 mm. The maximal MESHS of the category 1 hailstorms is 33 mm. The maximal MESHS of category 3 with a size of 50 mm is significantly larger than the maximal MESHS of category 1 and category 2. This result shows that the biggest hail stones are not triggered in the Napf region, but imported. Even if the path length, the lifetime and the area of the category 2 cells are all increased in comparison to the locally triggered category 1 cells, they do not produce bigger hail stones. This is surprising, since longer lifetime and path length generally lead to larger hailstone size (Schroeer, 2021). This holds only true for a comparison of the category 1 and the category 3 hailstorms in this analysis.
Still, it needs to be considered that MESHS and of course max MESHS are very uncertain variables when it comes to large grain sizes.

[C] Under which mesoscale conditions do hail events occur in the Napf region?

To answer this question, the locally triggered (category 1), and the imported hail cells from other regions (category 2 and 3) need to be treated separately.
Imported hail cells occur most often during a south-west weather type, a high, or a flat pressure distribution (see table 10). The ERA5 box plot analysis further reveales that imported hail cells occur on conditions with 13.9 to 14.1 m/s wind speed at 500 hPa in median. The difference in geopotential height from the north-western to the south-eastern edge of the domain, which is approximately 650 km, is 100 metres for

both categories 2 and 3 (figure 13 and 14). The bulk wind shear on days with imported hail cells is 10.7 m/s in median. Overall, categories 2 and 3 never show significant differences in the investigated environmental variables (chapter 3.4.1).

Locally triggered hail cells occur most often during a south-west weather type, a low, or a flat pressure distibution. However, the portion of low and flat weather distribution together results in a total of 72%. Hence, on 72% of the category 1 hail days, the wind speed at 500 hPa is below 7 m/s per definition. The wind speed at 500 hPa is with a median of 8.2 m/s for the locally triggered hail cells significantly lower than the 500 hPa wind speed of categories 2 or 3. This coincides very nicely with the results of the weather type analysis. In the ERA5 composite analysis (chapter 3.4.2), the geopotential height at 500 hPa shows a difference of 50 metres from the north-western to the south-eastern edge of the domain. This again shows that low wind speeds are expected at 500 hPa. The low wind speeds at 500 hPa imply that there is only a weak upper level air flow which leads to a slow displacement of the category 1 hail cells. The slow velocity of the category 1 hail cells leads to a short track length.
The bulk wind shear is a median 7.9 m/s for days with locally triggered hail (chapter 3.4.1). This is a significantly lower bulk wind shear than for days with imported hail cells. The ERA5 composite analysis shows lower bulk wind shear over the whole domain for category 1 than for categories 2 and 3. The case studies show that the bulk wind shear is lower for category 1 than for categories 2 or 3. The low vertical wind shear may not lead to the separation of the down and the updraft region. Hence, the formation of multicell and supercell storms is not possible under conditions with extremely low bulk wind shear. Following, I suspect the category 1 hailstorms to be mostly single cell hailstorms. However, a significant part of them is too long lived to be single-cell storms. For those long lived hailstorms, the interaction between storms may be important.
According to Wallace and Hobbs (2006), single-cell thunderstorms rarely produce hail because of a built-in "self-destruct-mechanism" namely, the downdraft circulation induced by the rain shaft. Weisman and Klemp (1986) state that severe weather, such as

high winds or hail may occur in single-cell storms but tends to be short-lived. Therefore, it is still poorly understood how hail can form in the locally triggered hail cells under very low bulk wind shear conditions. There is one aspect that may explain this phenomena, which is still under investigation (Schroeer, 2021): The MESHS signal is most likely overestimated for single-cell hailstorms, as it is assumed to be the case for the most of the category 1 hail cells. Hence, the locally triggered storms in reality produce smaller hail stones, or no hail stones at all. The MESHS is computed following the method of Waldvogel et al. (1979) and Foote et al. (2005) as discussed in chapter 2. Thus, the 45 and 50 dBz echo top height products and the freezing-level-height are used to calculate the MESHS. In the calculation it is not considered if a cell has been existing before or will continue to exist. The MESHS is assigned to a certain hail cell to a later point in time. In the assignment of the MESHS to a certain hail cell it is not considered whether it is a single, or a multi-cell storm.
This leads to an important limitation of this master thesis. As the hailstorms are determined by the TRT algorithm, only radar data is used. Thus, there is no evidence for hail on the ground. This limitation could be overcome by implementing data of the hail sensors in the Napf region, as they deliver ground observation of the hail events.

To close the circle, it needs to be addressed why the resampling models within the "Hail Climatology Switzerland" project do not fully capture the Napf hot spot. One the one hand, the resampling models build on hailstorms only, thus the relative frequency is not important for the resampling. On the other hand, the resampling uses large scale forcings. Local conditions are not included in the resampling. The findings of this thesis show that the local processes are important to describe the Napf hot spot, but it has still not been discovered how they interact.

6 Conclusion

The aim of this master thesis was to study the high frequency of hailstorms in the Napf region in Switzerland. Since the environmentally-driven resampling models that were developed within the "Hail Climatology Switzerland" project could not fully represent the Napf hot spot, it was of interest to assess the processes behind it.

The research of this master thesis, based on ERA5 reanalysis data and COSMO analysis data (chapter 2), compares locally triggered Napf hailstorms and Napf hailstorms imported from other regions (chapter 3.2) from 2002 to 2020. The ERA5 data analysis serves to get an overview of the meso-scale conditions during days with locally triggered hail cells versus days with imported hail cells. With the COSMO data, local scale phenomena were analyzed for selected case studies. Additionally, a relative frequency analysis was performed to investigate if only the number of hailstorms is increased in the Napf region or also the number of thunderstorms (chapter 4.2).

The relative frequency analysis showed with 5% a double as high relative frequency of hailstorms for the Napf region as for the reference regions. In the Napf region, 35% of the hail cells are locally triggered and 65% are imported. The analysis of the ERA5 data revealed that on days with locally triggered hail cells, the 500 hPa wind speed is significantly lower on the 5% level than on days with imported hail cells. Also, the bulk wind shear 850 to 500 hPa is significantly lower on days with locally triggered hail cells (chapter 4.5). The results of the COSMO case studies confirm the findings of the ERA5 analysis. They show a significantly lower bulk wind shear on days with locally triggered hail cells.

7 Outlook

In a further step, the COSMO case study analysis can be pursued by integrating the 10m wind data. By considering the 10m wind data, the first and the third hypotheses can be analyzed again in more detail.

In order to test the second hypothesis, the Napf region moisture availability from the boundary layer would need to be evaluated against the moisture content of the lower atmosphere in a similar, general setting of the northern Alpine pre-Alps without island-mountain topographies.

In this thesis, there is no separation of ordinary thermotopographic flow as alpine pumping and forced channel flow in the low-level boundary layer. This separation could be done in further work.

As discussed in chapter 5, hailstorms in the COSMO model may have developed earlier or later than in reality, or not at all. It would therefore be important to make a statement about how transient or stationary the conditions were during the case studies. This could be done by analyzing each case study for 5 hours. Starting two hours before the actual development of the hailstorm and ending two hours after it. With an extended case study analysis, it can be detected whether the conditions were stationary over several hours or if changes in, for example, the boundary layer height occurred once the hailstorm developed in the COSMO model.

The collected data of the hail pads in the Napf region could be used as evidence for hail on the ground. The hailstorms are determined by the TRT algorithm, hence there is no evidence for hail on the ground for these events.

To expand the analysis, a simulation of hail cells in the Napf region, for example by using a WRF model, could be consulted. An example application is the following: Analyze in a model environment the importance of the vertical wind shear in the Emme and Aare valley on locally triggered versus imported hail cells.

As introduced in section 1, the Napf region is a hail hot spot in Switzerland. But, the Napf region is only a part of a larger region with an increased number of hail days, see figure 21. By increasing the study region from the Napf region (red circle) to an

increased hot spot region (green circle), other processes might be found that may not be important for hail in the Napf region itself, but possibly for the hot spot region as a whole.

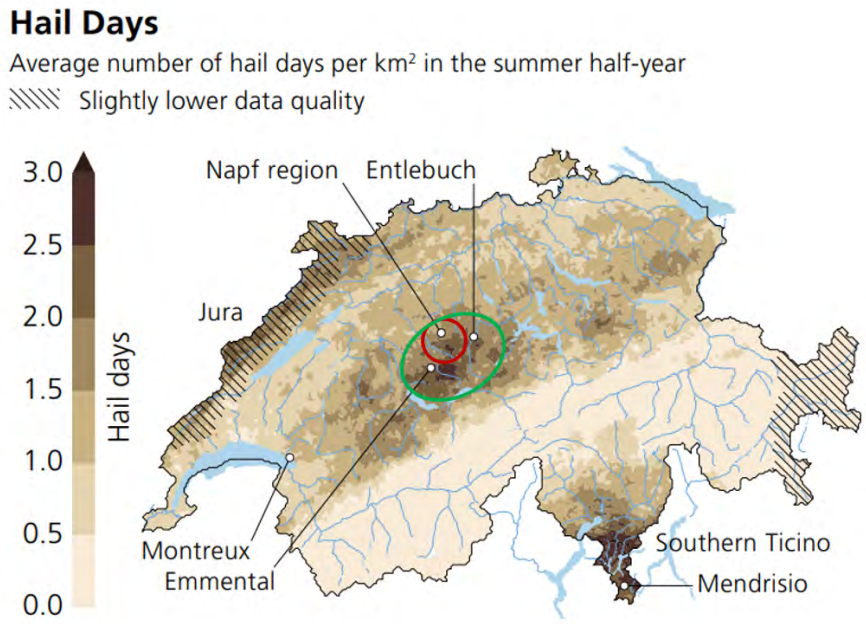

Figure 21: Napf region (red circle) and increased hot spot region (green circle).

Appendix

Category x < y		1 < 2	1 < 3	3 < 2	1 < 4	1 < 5	5 < 1
CAPE	pvalue	**0.01071**	**0.0356**	-	-	-	**0.0005**
	statistic	1'578	3'595	-	-	-	25'421
CIN	pvalue	no sign. difference between category 1-3			-	-	-
	statistic	-			-	-	-
T2M	pvalue	no sign. differences between category 1 - 5					
	statistic	-					
wind speed 500 hPa	pvalue	**0.0002**	**0.000005**	-	-	-	-
	statistic	1'113	2'655	-	-	-	-
wind speed 850 hPa	pvalue	**0.0156**	0.0754	0.1738	-	-	-
	statistic	1'399	3'729	2'133	-	-	-
bulk shear 850 - 500 hPa	pvalue	**0.0066**	**0.0006**	-	**0.0009**	**0.0169**	-
	statistic	1'335	3'073	-	43'498	27'943	-

Table A.1: P-values and test statistics of the Mann-Whitney-U significance tests for the box plots in figure 11. The p-values in bold show significant results on the 5% level.

Category x < y		**1 < 2**	**1 < 3**	**2 < 3**	**2 < 1**
Path length	pvalue	**0.0002**	**6.397 x 10-15**	**0.0009**	-
	statistic	1'351	2'074	1'941	-
Area	pvalue	0.0515	**7.374 x 10-11**	**1.959 x 10-5**	-
	statistic	1'775	2'645	1'664	-
Lifetime	pvalue	**0.0129**	**5.498 x 10-11**	**0.0011**	-
	statistic	1'643	2'627	1'960	-
max MESHS	pvalue	-	**7.379 x 10-12**	**1.042 x 10-11**	**0.0284**
	statsitic	-	2'496	1'715	938

Table A.2: P-values and test statistics of the Mann-Whitney-U significance tests for the storm characteristics in table 9. The p-values in bold show significant results on the 5% level.

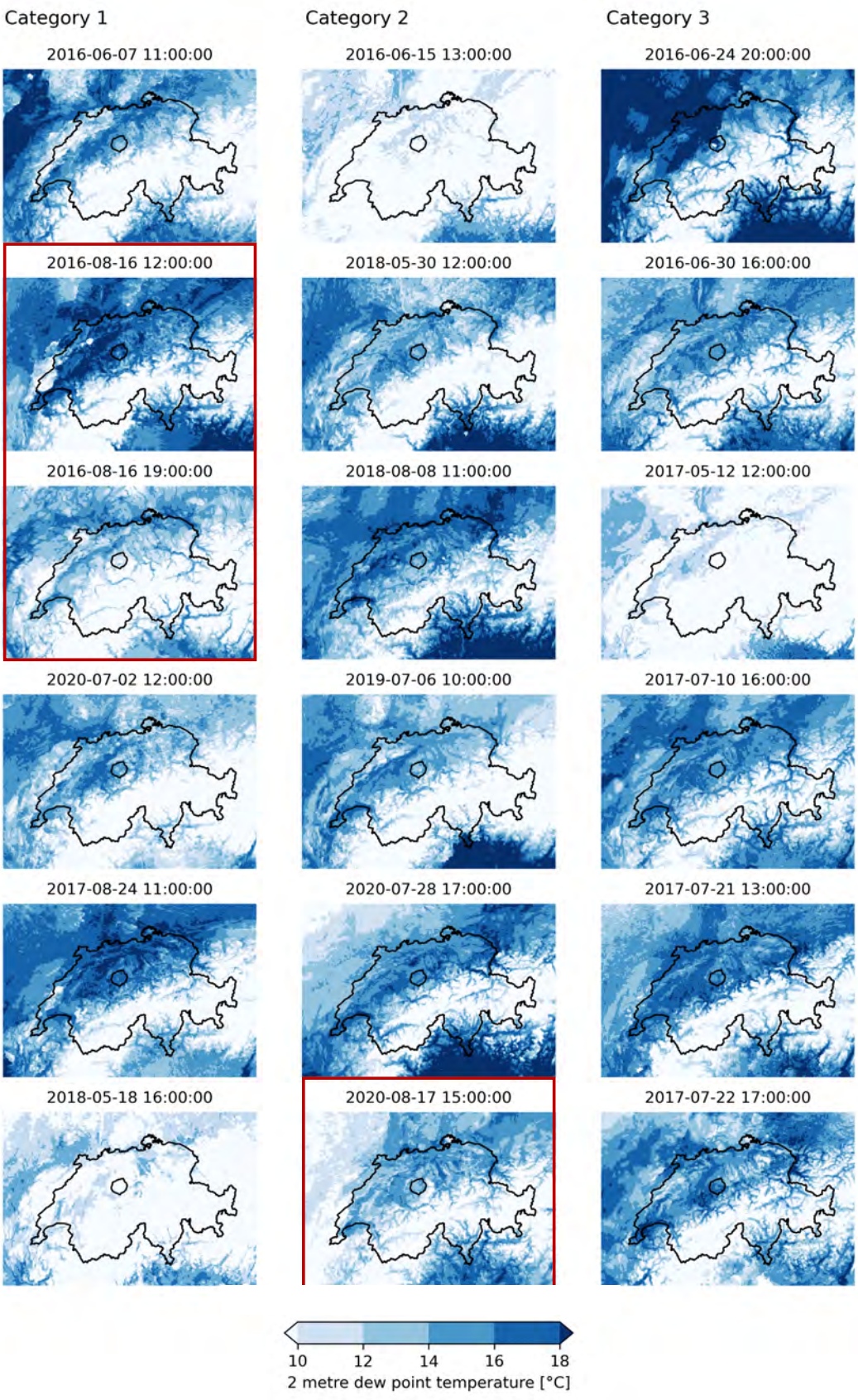

(a) Dew point temperature for case study 1-6 of each category

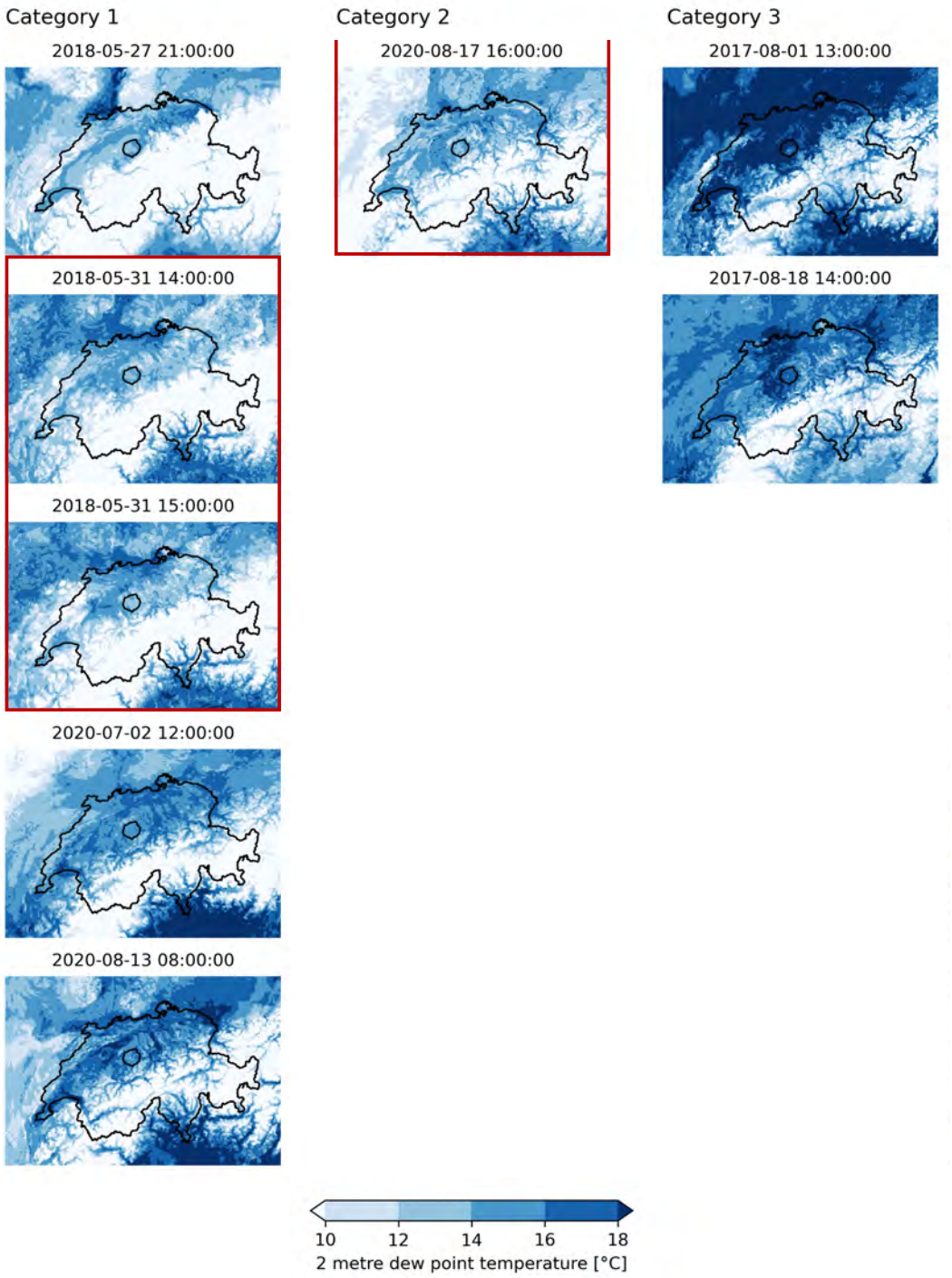

(b) Dew point temperature for case study 7-11 of each category

Figure A.3: Dew point temperature for all case study hailstorms. Time in UTC, one hour before the respective case study hailstorm was first detected. The red outline connects case studies occurring on the same day.

A.4 Transcript Interview

L = Luca Nisi; M = Marco Stoll; K = Katharina Schröer; U = Ursina Schwyn

Luca hat schon über den Napf gesprochen und dass es sicherlich mehrere Faktoren sind, die zu Hagel führen am Napf. Danach startet die Aufzeichnung:

M: Das ist sicherlich ein Zusammenspiel verschiedener Faktoren, die zu diesem Hotspot führen. Ein Teil des Hotspots ist einfach weil sowieso viele Gewitter da sind.

L: Im Napf was es eine homogene Verteilung der häufigen Relativität, als ich das einmal angeschaut habe.

M: ich finde die Fragestellung, die ihr anschaut (also ob die Hagelzellen einfach über den Napf drüber dampfen oder ob sich die intensivieren etc.) super. Also ob der Hagel importiert ist oder ob das local production ist.

U: zeigt plot mit einer Zelle darauf, wie sich die Geschwindigkeit ängert als die Zelle über dem Napf fährt

M: Die Geschwindigkeitszunahme der einen Zelle nach dem Napf ist ein Artefakt: es kann sein, dass sich eine Sekundärzelle am Nordrand des Napfes gebildet hat, oder das über dem Napf ein Splitting passiert ist. Der Algorithmus hat dann diese Tochterzelle (im Fall eines Splitting) der Mutterzelle angerechnet. Irgenetwas ist in der Natur passiert, das der Algorithmus so abgebildet hat aber es ist sicher nicht ein kohärentes Gewitter.

K: das war auch eine von Ursinas Fragen: die area der cellcenter sieht da auch ganz komisch aus.

M: TRT hat die Logik, dass bei einem Splitting der alte Track an den Neuen angehängt

wird. Also in bestimmten Situationen werden Mutter- und Tochterzelle zusammengehängt und in bestimmten Situationen nicht.

L: wenn es ein Splitting gibt hat man dieses Artefakt in der Geschwindigkeit weil es plötzlich eine Distanzverschiebung aufgrund einer neuen Zelle geben kann. Der Centroid ist positioniert über dem Pixel mit der höchsten Reflektivität. Die grösste Problematik hat man aber im Fall eines Splittings, wie Marco erklärt hat.

U: zeigt plot auf dem 3 Zellen mit der Geschwindigkeit drauf sind.

M: ich glaub bei der ganzen Geschichte mit der Geschwindigkeit würd ich glätten, vorsichtig sein, da würde ich nicht point for point interpretieren, weil die Geschwindigkeit, die im TRT drin steht, das sind die Punkte dieser Centroide. Die Gescheindigkeit eines Gewitters ist eigentlich die Summe aus 2 Komponenten: Motion und Propagation - unter Motion versteht man eigentlich das ganze Gebilde, die ganze Gewitterzelle, die Wolke und der Updraft und der Downdraft wird quasi passiv mit ambient wind transportiert (was auch immer das für ein Wind ist). Die zweite Komponente Propagation ist komplizierter, das ist wo entsteht der neue Updraft, die ganze 3D Dynamik von so einem Gewitter spielt da eine Rolle, wohin bewegt sich der Outflow, wo ist der Inflow am stärksten und das ganze wird dann wieder abgebildet im TRT, wo das TRT dann wiederderum einfach nur Reflektivität basiert ist. TRT schaut nicht wo ist ein Updraft oder ein Downdraft. Diese ganze Dynamik gibt es im TRT nicht. Darum würde ich vorsichtig sein die Geschwindigkeiten von diesen Zellen auf so feiner Zeit und Raumskala zu überinterpretieren, da lohnt sich ev ein bisschen eine Glättung.

L: Ja, absolut, ich hab selbst auch nicht viel mit der Geschwindigkeit gemacht wegen diesem Punkt. Die Positionierung des Centroids ist wirklich sehr nervös, vor allem für grössere Zellen. Natürlich - wenn die Zellen eine kleine Fläche haben ist es ein kleineres Problem. Ich habe versucht zu schauen prozentual wie viel Prozent der Hagelzelen macht ein Bewegung auf Basis der Trajektorie, die praktisch unmöglich

war, also musste ich eine starke Glättung machen damit diese komische Bewegung verschwindet. Man muss sicher eine starke Glättung machen aber mit der Gefahr, dass die Informationen plötzlich verschwinden werden, da man so stark glätten müsste.

M: nochmals zurück zu dem was Luca gesagt han, dem Inselberg. Das ist absolut richtig, der Napf ist schon etwas besonderes, wenn man ihn vergleicht mit den anderen Voralpen - sowohl auf der Nord- als auch auf der Südseite. Der Begriff Inselberg ist schon ziemlich gut. Wenn es darum geht zu überlegen warum gibt es dort so viele Gewitter und warum ist als Folge davon auch die Hagelhäufigkeit so gross. Ich stelle mir das ganze Hagelprodukt, das am Schluss am Boden ankommt als das Resultat von drei wichtigen Dingen vor: viel Wasser/Moisture, die transportiert wird - um dem Napf herum auf drei Seiten ist eigentlich flaches Terrain, sprich dort ist die Boundary Layer relativ dick und das verfügbare Wasser ist einigermassen gross, viellicht grösser als zum Beispiel in der Region Waadt, wo der Querschnitt zwischen Jura und Voralpen eher schmal ist. In der Region Luzern/Bern ist das Mittelland recht breit und die Masse an Wasser, die verfügbar ist ist relativ gross. Der Napf ist der Inselberg in der Mitte, der irgendwie mit seinen local Flows und mit Bise und mit Talwind, indem das alles so ein bisschen konvergent in die selben Spots saugt im Laufe des Tages. Das zweite Element ist mega entscheidend, wird oft bei Studien vernachlässigt - ist Concective Inhibition CIN. Der Napf als Inselberg, aber natürlich auch die ganzen Hügel rund herum, Beatenberg, Thun, diese ganzen Voralpengipfel helfen die CIN zu überwinden. Eine wichtige Rolle von diesen Inselbergen und den vorgelagerten Voralpen ist die Überwindung oder Minimierung von CIN in der Boundary Layer. Als Gegensatz dazu ist das Flachland , vor allem das östliche Flachland, das wirklich Flach ist, dort ist CIN häufig der Killer für Gewitter allgemein und auch für Hagel. Das könnte man sicher auch miteinbeziehen, was hat CIN für einen Effekt. Der dritte Punkt, dann sind wir dann wirklich beim Gewitter und nicht nur beim Hagel, ist Windshear. Irgendwie muss mitberücksichtigt werden, wenn wir den Link vom Gewitter allgemein zum Hagel machen wollen. Es ist immer die Frage welchen Windshear man überhaupt anschauen möchte in der Schweiz - möchte man einen lower boundary in der Boundary Layer drin

haben als untere Grenze um den Windshear zu beurteilen oder möchte man den Windshear midlevel beurteilen, dann müsste man irgendwie 2000/2500 meter bis 5000m, das weiss ich auch nicht was optimal ist um den Windshear zu beurteilen. Ich meine das ist etwas, das man allenfalls auch aus Reanalyse Daten wie ERA hinzunehmen könnte.

K: Ja das hab ich auch schon gemacht. Ich hab bei den ERA Daten da eher auf den höheren Levels (je weiter runter, desto schlechter repräsentiert ERA)

M: Ja genau, wenn du mit ERA arbeitest, musst du dich sowieso auf mid-level Windshear reduzieren, weil die Boundary Layer, das funktioniert einfach nicht in ERA auf der Skala, auf der die Gewitter funktionieren.

K: Ich mein ich hatte gar nicht so schlechte Korrelationen dazu, Ursina ich kann dir das mal geben.

M: beim Thema Windshear, da müsste man sich ein bisschen herantasten und ausprobieren. Da gibt es wahrscheinlich kein Rezept, das es schon gibt in der Literatur aus anderen Regionen, das man einfach so straight forward anwenden kann, weil die meisten Studien mit Hagel und Windshear, die sind über flat terrain und dort funktioniert die Superzellendynamik wie im Schulbuch. Selbst mit einer stündlichen COSMO Analyse ist es schwierig die Dynamik gut festzuhalten weil wir überall Berge haben, auch da wird man der Natur glaub nicht gerecht, mit dem Windfeld in der Boundary Layer und im Grenzbereich Boundary Layer und freie Troposphäre. Aber ich glaub eben diese drei Elemente muss man versuchen zu berücksichtigen - Moisture availability rund um den Napf - die Orographie, die das ganze Triggering und das overcome der CIN erleichtert - und die Windshear, die entweder synoptisch driven oder gar mesoscale irgendwie modifiziert wird durch das terrain. Ich hab mich schon paar mal gefragt, welche Rolle beispielsweise das Berner Aaretal spielt. Das ist eine ganz spannende Konfiguration weil das Aaretal ist quasi die Boundary Layer und da ist so ein Channel flow von Bern nach Thun, der ist immer Nord-West oder NNW tagsüber und darüber,

über der Boundary Layer ist oft WSW, allein diese konfiguration ist eigentlich - also da ist Windshear schon gegeben. Dasselbe ist nochmals ein Tal weiter, im Emmental hat man noch einmal die selbe Konfiguration. Jetzt kann man sich schon vorstellen, wenn ein Gewitter, das noch kein Hagel produziert aus den Fribourger Voralpen kommt und in diese sheared configuration hinein spaziert, das muss natürlich eine Auswirkung auf die Updraft helicity haben, wenn dort nur ansatzweise ein bisschen Luft aus der Boundary Layer hinein gelangt, in den Updraft, was nicht immer der Fall ist (manchmal ist die Boundary Layer völlig entkoppelt, und die Gewitter sind darüber hinweg) - aber das ist eine spannende Situation und das ist eben upstream vom Napf, diese Konfiguration mit Emmental und Aaretal, ich könnte mir vorstellen, wenn ihr dann feststellt, dass die meisten Hagelgewitter eben importiert sind am Napf, dass diese upstream configuration von Aaretal Emmental Boundary Layer, Alpine Pumping am Boden und SW-westerly synoptic flow darüber, dass das vielleicht ein Erklärungsansatz geben könnte für viele Napfgewitter, die nicht an Ort und Stelle schon entstehen.

L: Ja sicher, die Anwesenheit der Seen, auch wenn sie nicht besonders gross sind macht eine grosse Verfügbarkeit für feuchte Luft. Das kann man auch beim Lago Maggiore sehen, die Zellen überqueren den Lago Maggiore oft quer, weshalb es wie ein Wasserdampfstaubsauger gibt, wenn die Zellen den See überqueren, die viel Feuchte aufnehmen. So gibt es eine grosse latent heat release und eine sehr rasche Verstärkung der Gewitter. Das ist ein Grund warum auch die Gewitter über Luganese besonders stark sind, nicht wegen dem Lago Lugano aber weil die Gewitter aus W SW kommen und sie viel Feuchtigkeit mitnehmen. Das kann man wirklich auf dem Radar sehen, oft gibt es diese Explosionen und ich denke auch, dass die Gewitterzelle, die Simona analysiert war nicht über dem Napf, es gab ein Triggering in der Thun Region und sie hat dann der Aare nach Bern gefolgt. Man könnte jedoch in der Radaranimation sehen wie diese Zelle von der Bergenge über den See gegangen ist, es gab eine rasche Intensivierung der Zelle. Wie Marcco gesagt hat, dort gibt es eine Kombination von mehreren Elementen. Ich denke auch, dass dieses Tal besonders feucht ist an Sommertagen und die thermischen Winde bringen diese Feuchtigkeit Richtung der

Bergspitzen in der Napfregion. Man kann sehen, wie oft die ersten Zellen sich am Nachmittag entwickeln - einerseits dem Jura entlang, andererseits in der Napf Region. Es sind wirklich die frühen Zellen, die sich entwickeln. Für das Triggering ist die Windshear vielleicht nicht so wichtig, aber eine grosse Labilität und hohe Verfügbarkeit von feuchter Luft. Um eine Zelle in eine Hagelzelle zu entwickeln braucht man aber natürlich grosse Windshear. Sonst das ... (24:00) zersört die Gewitterzelle sehr schnell, was eigentlich in den Hochalpen passiert. In den Hochalpen gibt es oft Graupel wegen der tiefen Temperaturen und der tieferen relativen Feuchte aber eigentlich gross Hagel habe ich selbst im Nordtessin noch nie erlebt. Also wenn eine starke Gewitterfront kommt, gibt es vielleicht 1.5cm Hagel aber sonst wirklich Hagelschaden in den Alpen wurde sehr sehr selten gemessen.

M: vielleicht noch eine Ergänzung zum Einfluss der Seen. Das ist richtig, was Luca sagt, das ist natürlich eine gewisse Moisture Source aber ich glaub das ist erst in der zweiten Hälfte des Sommerhalbjahres wirklich wichtig. Beim Bodensee sieht man das ganz ganz krass. Immer von März bis Juni ist der Bodensee eigentlich eine Source of CIN weil er einfach kalt ist. Natürlich ist es auch eine Moisture Source aber der Effect von CIN wegen der kalten Oberfläche, der überwiegt am Anfang der konvektiven Saison. Irgendwann dann im Juli oder August kippt das Ganze auf die positive Seite, dann ist der See warm, Boundary Layer rund herum ist vielleicht nicht mehr ganz so warm und dann plötzlich ist die Moisture availability viel interessanter und wichtiger für die Gewitterbildung anstatt die Limitation, die sich aufgrund der Seetemperatur, also der inhibition ergibt.

K: Ja, ich denk mir sowas ist mega wertvoll. Die insights wenn man dann auch die verschiedenen Gruppen anschaut. Das lohnt sich da zu versuchen auseinanderzunehmen. Dann hat man irgendwie einen Grund anzunehmen, dass die dort verschieden sind, dann schauen wir mal erst nur die erste Hälfte der convective Season an und die zweite einzeln.

M: Ja also ich glaube die Diskussion mit den Seen, ich glaub beim Napf spielt das eher eine sekundäre Rolle.

K: Ursina, du hattest ja auch schon den lag zwischen Initialisierung und Hagel geplottet.

U: erklärt plot mit max MESHS und initiation Location drauf

M: kannst du irgendwie zwei Cluster daraus plotten, oder zwei Zentroide? Damit man sieht, der eine ist irgendwie upstream vom anderen. Das wär noch cool. Weisst du so in der Wolke ist es schwierig zu erkennen sind sie übereinander, oder sind sie von einander versetzt räumlich. Das könntest du mal ein bisschen ausprobieren, ob du irgendwie mit 80 Prozent von den Punkten einen Kreis darum fitten kannst und schauen ob die zentren verschieden sind oder nicht. Dann kommen wir der Frage schon ein bisschen auf die Spur - ist das eigentlich hausgemacht oder ist das importiert.

L: Ich erinnere mich, dass ich einmal einen Vergeich gemacht habe über der Alpennordseite - das heisst ich hatte die Klimatologie der Starksniederschlagakkumulation immer mit Radar - ich habe glaube ich 30mm/h genommen und ich habe mit POH 80 gemacht - und ich erinnere mich, der erste Hotspot war mehr in Richtung der Freiburger Alpen und der zweite war wirklich der Napf. Deswegen hatte ich dann dort die Frage ok berechnen wir die relative Häufigkeit der Hagelstürme zu der totalen Anzahl der Gewitter. Aber ich erinnere mich an diese Differenz: Für Starkregen es gab wirklich diesen Hotspot mehr Richtung Freiburgische Alpen und ein bisschen nur über dem Napf und genau umgekehrt für Hagel. Aber ich hatte dann die Gründe nicht weiter analysiert. Dieser zweite Hopspot war wirklich weit vom Napf weg, der für starken konvektiven Regen. Vielleicht könnte es sein, dass die beiden Hopspots unabhängig von einander sind, das heisst die Gewitter, die der erste Hotspot produziert sind nicht die selben, die den zweiten Hotspot treffen. Ich habe versucht die Grafik zu finden aber ich finde sie nicht.

M: Also das ist schon mal ein cooler Plot hier. Inititation and max MESHS location.

K: sinngemäss: Wenn man das klimatologisch anschaut, hat man immer recht viel auf einmal. Wir müssen die wichtigen Dinge noch etwas rausarbeiten.

M: habt ihr schon mal Cluster gemacht? Habt ihr die Trajektorien von diesen Napf hailstorms mal versucht irgendwie zu clustern?

U: Ich habs versucht aber war noch nicht erfolgreich.

K: Ich hab für die gesamten recht viel mit den Cluster gemacht aber nicht spezifisch für den Napf. Das wär jetzt der nächste Schritt, dass wir die Napfzellen in die verschiedenen Kategorien einteilen, die wir bereits für die Gesamtschweiz haben. Im resampling wird auch berücksichtigt ob es eher die langlebigen oder lokal stationäre, kurzlebige Zellen sind, die eben interessanterweise auch ziemlich unterschiedliche MESHS Verteilungen haben. Wobei wir ja auch alle wissen, dass das MESHS nicht unbedingt das realitätsnähste ist.

M: Das ist halt einfach das, was man hat. Ich mein das ist schon gut.

K: Ja genau. Man muss manche Sachen einfach mit Vorsicht geniessen. Es zeigen sich - also wenn sich innerhalb ist das MESHS ja immer das gleiche und wenn sich dann dort ziemlich signifikante Unterschiede ergeben weiss man trotzden was über den Unterschied. Das wär jetzt der Plan - also wir sehen jetzt schon, dass es ja verschiedene Kategorien zu geben scheint mit dem importiert und hausgemacht und das man die nun von einander trennt und dann die Plots auch für die verschiedenen Cluster macht.

M: Ja, das wär cool. Und eben versuchen auch rauszufinden gibt es vielleicht einen Unterschied, einen Cluster, der - ich fantasiere jetzt: der aus den Fribourger Voralpen

kommt und der vielleicht mehr Hagel produziert und ein anderer der eher aus Westen kommt, also aus dem Berner Mittelland, der vielleicht weniger Hagel produziert oder umgekehrt, keine Ahnung, das ist jetzt nur daher philospohiert. Also irgend solche Differenzen versuchen herauszufinden würde einen auf die Spur bringen um die Prozesse zu verstehen denke ich.

L: Ich habe etwas gefunden, ich teile mal den Bildschirm. Weil ich hab es vorhin nicht korrekt gesagt. Das war eine alte Präsentation, ich denke es war 2014 oderso. Ja ich hatte diese Klimatologie gemacht, eigentlich war die Correlation? grösser als 25mm und es sind zwei Hotspots. Aber besonders war, dass der Hagelhotspot wirklich nur über dem Napf zu sehen war und nicht der erste. Aber wie gesagt, ich hatte dann nicht weiter analysiert für die Alpennordseite. Im Süden gab es auch diese Differenz, diese typische konvektive Linie und prefrontale Situationen dann die normale Gewitterhäufigkeit mit Maximum über dem zentralen/südlichen Tessin. Aber eigentlich kann man sehen, dass das die relative Häufigkeit ein bisschen bestätigt von Hagelstürmen. Die ist nicht besonders hoch, auch wenn ein Hotspot für starke konvektive Niederschläge ohne Hagel da war. Die Hagelphänomene wurden aus dem Datensatz herausgenommen, das ist nur Wasser, das auf dieser Differenz (links) zu sehen ist. Ich hab das wie gesagt nicht weiter analysiert, nur einige Hypotesen dazu gemacht.

M: Luca, das ist der Saanenland CB den wir hier sehen (linkes Bild gelb eingerahmt). Das ist der Fringerpring vom Saanenland CB. Den gibt es immer nach einer Phase - 1, 2 oder 3 Tage Hochdruck und Temperaturaufbau. Einer der ersten CB's die es gibt, wenn man eigentlich schon fast gar nicht damit rechnet ist in diesem Spot in der Region Gstaad und der kommt manchamal am selben Tag wie derjenige am Lac de Joux im westlichen Jure, der kommt immer wenn die Hochdruckgebiete langsam abgebaut werden und die instability so ganz ganz langsam zunimmt, meistens reicht es dann noch um 4,5,6 Uhr abends für einen isolated thunderstorm in der Region Sannenland. Das kommt so häufig vor, diese Wetterlage, dass das wahrscheinlich in deiner Statistik hier diesen Fingerpring hinterlässt. Er ist immer am selben Ort.

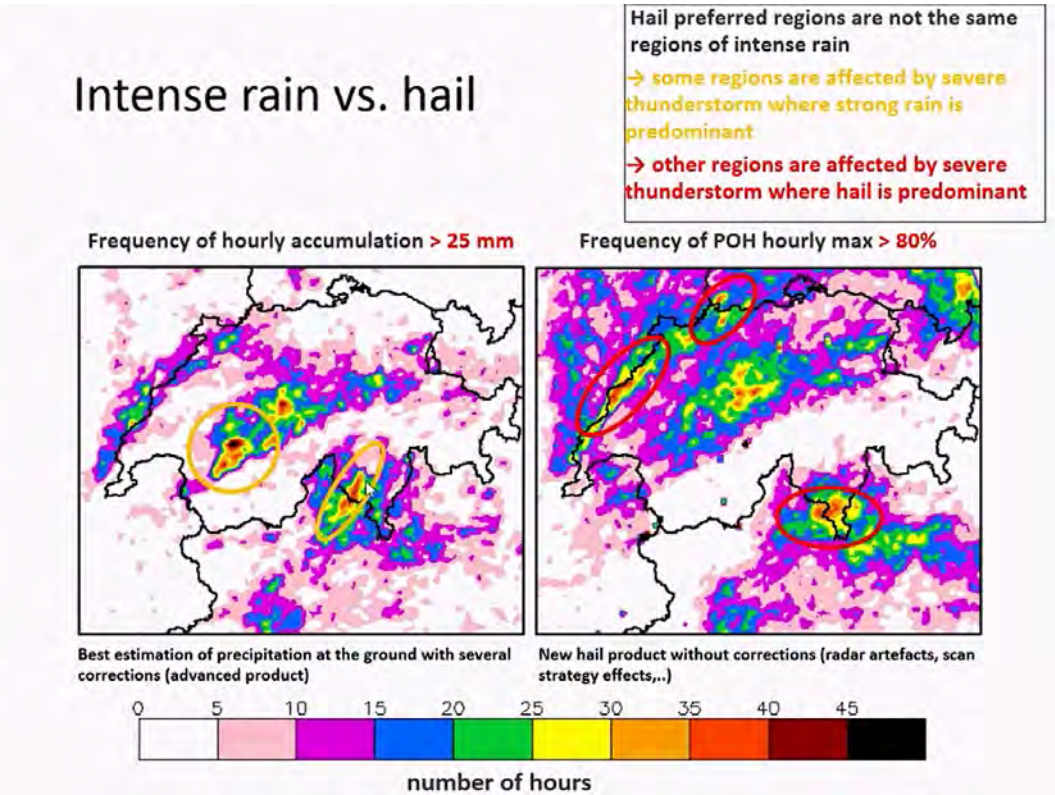

L: aah, oke, das ist interessant

M: es erstaunt mich jetzt nicht, dass dieser Spot auf dem Bild rechts nicht mehr auftaucht, weil das ist ja dann eine ganz andere Wetterlage als wenn am Napf die Hagelgewitter auftauchen. Typischerweise ist das ein low-windshear Regime, eher ein flash-flood Regime, das aber nur marginal instabil ist.

K: Das ist jetzt im Eigenintersse für unseren Hagel; es gibt die Hagelkarte vom schweizer Hagel, da hat die einen Hotspot, der von da kommt denk ich. Die Leute sagen dann immer ja da ist nichts, da hagelt es nie sagen die Leute, die mit den Schäden da zu tun haben und jetzt hast du ja eigentlich ne Erklärung geliefert.

L: Ja genau, weil in dieser Karte haben sie auch Radardaten verwendet, nicht wirklich Hagelprodukte, das ist der Grund dafür.

K: Wir müssen jetzt rechtfertigen wenn die neuen Hagelkarten rauskommen müssen

wir sagen wiso das jetzt eine der Diskrepanzen ist.

M: Also wenn sie euch das nicht glauben, dann können wir euch gerne helfen. Das kann man synoptisch-dynamisch sehr gut erklären.

L: Ich hatte auch andere Fragen gelesen, die du Ursina gesendet hast, einige waren ziemlich schwierig. Ich denke auch Marco - ich muss das noch öffnen, was du gestern geschickt hast.

U: Ja vielleicht nochmals zu den Trigger von den Hagelzellen selbst. Ich hab jetzt noch mal ein Bild geteilt: darauf sieht man auch - also es von allen Seiten her diese Talwinde aber der rote Kreis, den man sieht, das ist ja eigentlich schon das Tal, auf der Seite sind ja dann schon wieder die Hügel. Der meiste Wind kommt von Westen aber die Verteilung der ersten Detektion der Hagelzellen ist ja eigentlich doch ziemlich verteilt rund um den Napf herum und geht dann sozusagen von allen Seiten auf den Napf zu. Wie kann man das erklären?

L: Das ist nur mit Westwinden? Also hast du die Grosswetterlagenklassifikation verwendet?

U: Das sind jetzt alle.

L: Ok, vielleicht - das ist schwierig zu interpretieren. Das muss man im Clustering machen.

K: Ursina, du hattest die Tracks doch auch nach Wetterlage eingezeichnet. Also nicht die Initialisierungspunkte aber die Tracks.

U: zeigt Grafik mit Trajektorien nach Wetterlage

M: mmh, nach Wetterlage, cool! Das ist aber geil, die hab ich gar nicht gesehen vorher, sorry.

U: ah, da bin ich vorher schnell drüber

M: Ja, der ist spannend, der ist cool. Ich mach grad einen Screenshot von dem. Ich brauch den für meine Schulung.

K: Marco, ich hab dies sonst auch von allen Jahren, vielleicht sollte ich mal das Repository aufmachen von den ganzen Trajektorienplots, die wir da haben.

M: Da gibt es ein paar ganz seltsame Kerle. Der eine, der da von Bellinzona über die Alpen geht, der ist sehr speziell. Den glaub ich ehrlich gesagt nicht.

K: Man sieht schon, dass wenn man die anschaut, vor allem im Wallis - dieses Alpenbogen-Minimum, das wird schon öfters durchbrochen auf dem Kanal, wo man jetzt die vier, die da grad noch reinreichen - das sind jetzt nur die Tracks, die die Napf Region schneiden im Laufe ihrer Zeit. Aber wenn man das jetzt ein bisschen weiter rechts nehmen würde im Osten, gibt es doch einige, die da diese Bahn über den Gotthard oder was da ist nehmen. Die da dieses Alpenminimum durchbrechen.

M: Ja gut, so viele sind das nicht. Aber es gibt schon ein paar die das erstaunlicherweise tun. Aber die meisten setzen allerhöchstens am Alpenkamm an oder nördlich davon.

K: Ja, die könnten wir mal rausplotten, alle die da oben.

M: Es sind nur zwei so ganz merkwürdige Typen, die über die Alpen hindurchgehen.

K: Aber das sind ja jetzt nur die, die den Napf kreuzen, aber ich mein insgesamt von denen. Aber ich mein hat das vielleicht schon - ihr habt ja auch gesagt, dass es wie dann - es gibt das Teil im Westen und im Osten und wenn dass dann sozusagen das durchbricht dann Ursina also du siehst ja, dass die im Westen bei deinen Initialisierungspunkten nach Westen streuen sie viel weiter aus als nach Osten und von Osten sinds wahrscheinlich dann eher die lokalen.

M: Habt ihr mal etwas herumgespielt mit den Intensitäten? Ein Vergleich mit Weathertypes und Intensität? Also mal zruück auf Feld 1 - ab wann habt ihr einen hailstorm als hailstorm klassifiziert? Ab MESHS über 1cm?

K: MESHS ist ab 2cm definiert und wir haben jetzt die MESHS, also es gibt wie immer entweder du nimmst alle Gewitterzellen, dann die POH 80 werden ja noch - Luca, du hast auch oft die POH 80 genommen oder und dann die mit MESHS als sozusagen die Intensiven. Wir haben jetzt auch mit den ganzen Stakeholdern festgestellt, dass wenn es ein MESHS Signal gibt, dann gibt es doch meistens auch Hagel, während POH 80, vor allem auch in der Fläche was sagt, aber dass sie es als intensiven Sturm oder Gefährdung wahrnehmen.

M: Habt ihr auch Kriterien wie häufig? Also über wie viel Zeitdauer eine Gewitter eine gewisse Intensität haben muss?

U: Wir haben einfach festgelegt, dass das Gewitter insgesamt mindestens 15min dauern muss und eben die MESHS auf 20, aber nicht dass jetzt die MESHS über 10 Minuten so und so hoch sein muss, das haben wir nicht drin.

M: Nur das ich weiss wie es definiert ist. Wenn man das weiss, dann kann man es auch interpretieren.

K: Aber das wär sicher auch was, dann noch die ganz intensiven, oder die die über

ihre Zeitdauer halt auch viel Hagel haben - das ist jetzt halt der Unterschied, es gibt ja oft auch diese Zellen, die so Impulse haben, die hüpfenden.

M: Ja genau, darauf wollte ich heraus. Ich meine es gibt schon auch Hagelellen oder Gewitterzellen, die einfach einmal kurz, für ein oder 2 TRT Zeitpunkte kurs ihre Hagelfracht deponieren aber das wars dann auch schon. Und ein bisschen böse gesagt kann man sagen ja gut, das ist irgendwie auch Teil der normalen Gewittervariabilität, aber wahrscheinlich seid ihr vermutlich eher an denen interessiert, die so eine viertel oder halbe Stunde lang eine gewisse Hagelintensität erreichen. Oder nein, vielleicht kann man es anders formulieren: dieser kurze Hagelpuls, den es wahrscheinlich oft gibt könnte man vielleicht noch einmal versuchen zu separieren von denjenigen Hagelstürmen, die vielleicht eine halbe Stunde oderso eine gewisse Hagelstärke produziert. Ich mein das wären so kleine, so Filterübungen mit dem Datensatz, den man eh schon hat, das Plotskript wird wahrscheinlich immer das selbe sein und man kann ein bisschen rumspielen indem man den ganzen Datensatz, der dahintersteckt einfach ein bisschen einschränkt auf die eine oder andere Art und Weise ob man dort irgend welche Auffälligkeiten findet. Wenn du nochmals zurück gehst auf diese Punktdarstellung von den Initiation points - ich bin recht erstaunt, wie viele Punkte doch nördlich und östlich des Napfs stehen. Das hätte ich jetzt nicht erwartet.

U: Ja aber das muss ich wirklich mal noch plotten mit der Zugrichtung um zu sehen, wenn die da von Westen kommen, ob die dann wirklich westlich des Napfs getriggert werden.

M: Ja. Also ich hätte jetzt intuitiv nicht gedacht, das jetzt so viele auch von Norden her kommen, also vom Aargau und von der Region Zürich sogar.

K: Du könntest ja dann eh auch noch die Initialisierung mit den Clustern, wo sie herkommen nochmals anschauen.

M: Hier könntest du auch, den Plot könntest du zum Beispiel auch mit farbigen Punkten noch machen, indem du irgendwie versuchst verschiedene Intensitäten oder andere Lifecycles zu unterscheiden. Die kurzlebigen Hagelpulse, diese einmaligen mit einer anderen Farbe zeichnest als diejenigen, die 30 min oder länger Hagel produzieren.

U: Ja oder wir haben auch gedacht einen Dichteplot zu machen, weil jetzt ist es schwierig zu sehen, wie viele mehr denn wirklich da am Napf entstehen, weil es sieht nach viel aus, auch in der Region Zürich aber doch extrem viel mehr beim Napf.

M: Jaja genau, man weiss nicht wie viele es wirklich da am Napf sind, das geht irgendwie unter, das stimmt, ein Dichteplot wäre nicht schlecht. Aso ich denk, da könnt ihre mit den bestehenden Daten und den Skripten, die ihr eh schon habt recht viel mal so niederschwellig noch mit Filtern und mit Strukturieren der Daten könnt ihr viel einfach mal testen und ausprobieren, ob sich da was ergibt. Und eben das ganz Clustering der Tracks fände ich recht interessant, ich könte mir vorstellen, dass man da was lernen würde. Ich glaube du kannst jetzt mal zwei drei Schritte machen und uns dann wieder mal treffen in ein paar Wochen oder je nach dem wie schnell du Fortschritte machst, können wir gerne so ein Meeting mal wiederholen. Ich würd sehr gerne da ein bisschen mitschauen und mitdenken und mithelfen, ich möchte euch nicht zu viel dreinreden, aber ich kann sehr viel lernen dabei aus diesen Statistiken.

U: Ja sehr gerne, wir können auch viel lernen. Jetzt noch bezogen auf - also wir haben ja gesagt, dass die Boundary Layer relativ dick ist beim Aaretal - die moisture Daten aus dem ERA sind wahrscheinlich auch zu grob, das müsste man eher mit den COSMO Daten anschauen

M: Ja, das ist zu grob, das braucht mindestens COSMO Analysen. Ich mein die Schwierigkeit wenn man Modellanalysen nimmt ist halt immer, im gegensatz zur Natur, ich mein in der Natur unterscheidet man das preconvective Environment, das ist quasi alles bei ungestörter Situation und dann kommen irgendwann diese Gewitter und

nacher ist alles nur noch Chaos. Das ist cold pools und Chaos und alles ist anders als vorher. Ob das in reanalyse Daten immer so perfekt wiedergegeben ist, selbst wenn man COSMO Reanalysen nimmt, bin ich mir nicht 100% sicher. Natürlich, man kann sich wieder auf den Standpunkt stellen wir haben nichts besseres, also nehmen wir COMSO Analysen. Das ist zumindest von der Orographie her und der Modelldynamik, die dahinter steckt, ist das einfach das Beste, das wir haben, also gut, nehmen wir das. Trotzdem muss man sich die Frage irgendwann stellen, ist so eine Dynamik einer konvektiven Situation wo ein sauberes preconvective Environment bereit ist und quasi so ein Teil der Ursache bildet für ein Hagelgewitter, ist das wirklich in den Reanalysedaten so drin. Das ist immer so ein bisschen das Fragezeichen wenn man mit Reanalysedaten arbeitet.

L: Ja absolut. Das ist die schwierigste Frage um sicher zu sein, was nimmt jetzt eigentlich ein echtes preconvective environment und nicht schon von den Stürmen, die vieleicht [ein wort] gestört sind. Ich denke dort hat auch Simona Trefalt ein bisschen Schweirigkeiten gehabt, wenn sie diese COSMO Analysen genommen hat. Das war nicht so einfach, vor allem in einer automatischen Weise grosse Datensätze von COSMO zu analysieren und sicher zu sein, dass nicht schon Stürme die Umgebungen beeinflusst haben drin waren.

M: Gerade das COSMO war eingentlich jahrelang berühmt dafür, dass es das convective Triggering viel zu früh, 2-3h zu früh, modellisiert. Das hat jahrelang jede Verifikation gezeigt, dass convective Precipitation over orography im Sommer immer 2-3h zu früh passiert ist und im Prinzip hat das Modell sich dann schon selber ein bisschen das convective Environment versaut oder modifiziert mindestens. Mit der 2km Auflösung wurde es ein bisschen besser, also wenn man auf der convection permitting Skala geht, ist der Effekt nicht mehr ganz so dramatisch aber er ist immer noch ein Stück weit vorhanden.

List of Figures

List of Tables

References

Adams, W. (2015). *Conducting Semi-Structured Interviews*.

AMS, A. M. S. (2021). nonhydrostatic model. https://glossary.ametsoc.org/wiki/Nonhydrostatic$_m$*odel*.

BAFU Bundesamt für Umwelt (2016). Umgang mit Naturgefahren in der Schweiz - Bericht des Bundesrats in Erfüllung des Postulats 12.4271 Darbellay vom 14.12.2012. Technical report.

Barras, H., Hering, A., Martynov, A., Noti, P.-A., Germann, U., and Martius, O. (2019). Experiences with >50,000 Crowdsourced Hail Reports in Switzerland. *Bulletin of the American Meteorological Society*, 100(8):1429–1440.

Bluestein, H. B. (1993). Synoptic-dynamic meteorology in midlatitudes. volume ii. observations and theory of weather systems.

Brooks, H. E., Anderson, A. R., Riemann, K., Ebbers, I., and Flachs, H. (2007). Climatological aspects of convective parameters from the NCAR/NCEP reanalysis. *Atmospheric Research*, 83(2):294–305.

Bunkers, M. J. (2002). Vertical wind shear associated with left-moving supercells. *Weather and Forecasting*, 17(4):845 – 855.

Davies, J. M. (2004). Estimations of cin and lfc associated with tornadic and nontornadic supercells. *Weather and Forecasting*, 19(4):714 – 726.

Davies, J. M. and Johns, R. H. (1993). *Some Wind and Instability Parameters Associated With Strong And Violent Tornadoes: 1. Wind Shear And Helicity*, pages 573–582. American Geophysical Union (AGU).

de la Torre, A., Pessano, H., Hierro, R., Santos, J., Llamedo, P., and Alexander, P. (2015). The influence of topography on vertical velocity of air in relation to severe storms near the southern andes mountains. *Atmospheric Research*, 156:91–101.

Doms, G. and Baldauf, M. (2021). A Description of the Nonhydrostatic Regional COSMO-Model. page 168.

Doswell, C. A. (1987). The distinction between large-scale and mesoscale contribution to severe convection: A case study example. *Weather and Forecasting*, 2(1):3 – 16.

Doswell III, C., Brooks, H., and Maddox, R. (1996). Flash flood forecasting: An ingredients-based methodology. *Weather and Forecasting*, 11:560–581.

ECMWF (2021). Parameter Details. https://apps.ecmwf.int/codes/grib/param-db?id=228001, Accessed:17.12.2021.

Foote, B., Krauss, T., and Makitov, V. (2005). Hail metrics using conventional radar. *85th AMS Annual Meeting, American Meteorological Society - Combined Preprints*.

Frei, C. (2020). Lecture slides: Analyses of Climate and Weather Data.

Hering, A. (2018). TRT (Thunderstorms Radar Tracking). page 8.

Hering, A. M., Germann, U., Boscacci, M., and Sénési, S. (2008). Operational nowcasting of thunderstorms in the Alps during MAP D-PHASE. page 6.

Hering, A. M., Morel, C., Galli, G., Senesi, S., Ambrosetti, P., and Boscacci, M. (2004). Nowcasting thunderstorms in the Alpine region using a radar based adaptive thresholding scheme. page 6.

Hersbach, H., Bell, B., Berrisford, P., Hirahara, S., Horányi, A., Muñoz-Sabater, J., Nicolas, J., Peubey, C., Radu, R., Schepers, D., Simmons, A., Soci, C., Abdalla, S., Abellan, X., Balsamo, G., Bechtold, P., Biavati, G., Bidlot, J., Bonavita, M., De Chiara, G., Dahlgren, P., Dee, D., Diamantakis, M., Dragani, R., Flemming, J., Forbes, R., Fuentes, M., Geer, A., Haimberger, L., Healy, S., Hogan, R. J., Hólm, E., Janisková, M., Keeley, S., Laloyaux, P., Lopez, P., Lupu, C., Radnoti, G., de Rosnay, P., Rozum, I., Vamborg, F., Villaume, S., and Thépaut, J.-N. (2020). The ERA5 global reanalysis. *Quarterly Journal of the Royal Meteorological Society*, 146(730):1999–2049. _eprint: https://rmets.onlinelibrary.wiley.com/doi/pdf/10.1002/qj.3803.

Joe, P., Burgess, D., Potts, R., Keenan, T., Stumpf, G., and Treloar, A. (2004). The s2k severe weather detection algorithms and their performance. *Weather and Forecasting*, 19(1):43 – 63.

Johns, R. H. and Doswell, C. A. (1992). Severe local storms forecasting. *Weather and Forecasting*, 7(4):588 – 612.

Kaltenböck, R., Diendorfer, G., and Dotzek, N. (2009). Evaluation of thunderstorm indices from ecmwf analyses, lightning data and severe storm reports. *Atmospheric Research*, 93(1):381–396. 4th European Conference on Severe Storms.

Kunz, M. and Puskeiler, M. (2010). High-resolution assessment of the hail hazard over complex terrain from radar and insurance data. *Meteorologische Zeitschrift*, 19(5):427–439.

Lellig, C., Graf, O., and Moser, S. (2014). Kommunikation fir einen wirksamen Gebäudeschutz. Schlussbericht zur 7. Ausschriebung der Präventionsstiftung der Kantonalen Gebäudeversicherungen KGV, Bern.

Madonna, E., Ginsbourger, D., and Martius, O. (2018). A Poisson regression approach to model monthly hail occurrence in Northern Switzerland using large-scale environmental variables. *Atmospheric Research*, 203:261–274.

Mann, H. B. and Whitney, D. R. (1947). On a Test of Whether one of Two Random Variables is Stochastically Larger than the Other. *The Annals of Mathematical Statistics*, 18(1):50 – 60. Publisher: Institute of Mathematical Statistics.

MeteoSwiss (2021). Hail climatology. https://www.meteoswiss.admin.ch/home/climate/swiss-climate-in-detail/hail-climatology.html.

MeteoSwiss (2021). Hail Climatology. https://www.meteoswiss.admin.ch/home/climate/swiss-climate-in-detail/hail-climatology.html, Accessed:18.10.2021.

Mohr, S., Kunz, M., and Geyer, B. (2015a). Hail potential in Europe based on a regional climate model hindcast: HAIL POTENTIAL IN EUROPE. *Geophysical Research Letters*, 42(24):10,904–10,912.

Mohr, S., Kunz, M., and Keuler, K. (2015b). Development and application of a logistic model to estimate the past and future hail potential in Germany: LOGISTIC MODEL ESTIMATING HAIL POTENTIAL. *Journal of Geophysical Research: Atmospheres*, 120(9):3939–3956.

NCCS (2021). Hail climate switzerland. https://www.nccs.admin.ch/nccs/en/home/the-nccs/priority-themes/hail-climate-switzerland.html.

NCCS National Center for Climate Services (2021). Hailstone sizes. https://www.nccs.admin.ch/nccs/en/home/the-nccs/priority-themes/hail-climate-switzerland/hailstone-sizes.html, Accessed:18.10.2021.

Nisi, L., Hering, A., Germann, U., and Martius, O. (2018). A 15-year hail streak climatology for the Alpine region. *Quarterly Journal of the Royal Meteorological Society*, 144(714):1429–1449.

Nisi, L., Martius, O., Hering, A., Kunz, M., and Germann, U. (2016). Spatial and temporal distribution of hailstorms in the Alpine region: a long-term, high resolution, radar-based analysis: Spatial and Temporal Distribution of Hailstorms in the Alpine Region. *Quarterly Journal of the Royal Meteorological Society*, 142(697):1590–1604.

Nisi, L. and Stoll, M. (2021). personal interview.

Punge, H. and Kunz, M. (2016). Hail observations and hailstorm characteristics in Europe: A review. *Atmospheric Research*, 176-177:159–184.

Rotach, M. W., Ambrosetti, P., Ament, F., Appenzeller, C., Arpagaus, M., Bauer, H.-S., Behrendt, A., Bouttier, F., Buzzi, A., Corazza, M., Davolio, S., Denhard, M., Dorninger, M., Fontannaz, L., Frick, J., Fundel, F., Germann, U., Gorgas, T., Hegg, C., Hering, A., Keil, C., Liniger, M. A., Marsigli, C., McTaggart-Cowan, R., Montaini, A., Mylne, K., Ranzi, R., Richard, E., Rossa, A., Santos-Mu?oz, D., Sch?r, C., Seity, Y., Staudinger, M., Stoll, M., Volkert, H., Walser, A., Wang, Y., Werhahn, J., Wulfmeyer, V., and Zappa, M. (2009). MAP D-PHASE: Real-Time Demonstration of Weather Forecast Quality in the Alpine Region. *Bulletin of the American Meteorological Society*, 90(9):1321 – 1336. Place: Boston MA, USA Publisher: American Meteorological Society.

Schemm, S., Nisi, L., Martinov, A., Leuenberger, D., and Martius, O. (2016). On the link between cold fronts and hail in Switzerland: On the link between cold fronts and hail in Switzerland. *Atmospheric Science Letters*, 17(5):315–325.

Schroeer, K. (2021). personal message.

Sturmarchiv Schweiz (2019a). 20090723 01 Hail Mezieres FR.

Sturmarchiv Schweiz (2019b). 20090723 02 Hail Burgdorf BE.

Sturmarchiv Schweiz (2021). Sturmarchiv Schweiz - Swiss Severe Weather Database (SSWD). https://www.sturmarchiv.ch/, Accessed:15.08.2021.

Torriani-Braga, Y. (2009). ein verheerender Hagelschlag. *Die Zeitschrift der Schweizerischen Hagelversicherungs-Gesellschaft*, 3:6–7.

Trefalt, S. (2017). *Hail and Severe Wind Gusts in the Convective Season in Switzerland*. PhD thesis.

Trefalt, S., Martynov, A., Barras, H., Besic, N., Hering, A. M., Lenggenhager, S., Noti, P., Röthlisberger, M., Schemm, S., Germann, U., and Martius, O. (2018). A severe hail storm in complex topography in Switzerland - Observations and processes. *Atmospheric Research*, 209:76–94.

Treloar, A. (1998). Vertically integrated radar reflectivity as an indicator of hail size in the greater sydney region of australia. In *Preprints, 19th Conf. on Severe Local Storms, Minneapolis, MN, Amer. Meteor. Soc*, pages 48–51.

VKF (2013). Naturgefahren und Prävention innerhalb der VKF. Technical report.

Waldvogel, A., Federer, B., and Grimm, P. (1979). Criteria for the Detection of Hail Cells. *Journal of Applied Meteorology and Climatology*, 18(12):1521 – 1525. Place: Boston MA, USA Publisher: American Meteorological Society.

Wallace, J. M. and Hobbs, P. V. (2006). *Atmospheric science: an introductory survey*. Number v. 92 in International geophysics series. Elsevier Academic Press, Amsterdam ; Boston, 2nd ed edition. OCLC: ocm62421169.

Weisman, M. L. and Klemp, J. B. (1984). The structure and classification of numerically simulated convective stormsin directionally varying wind shears. *Monthly Weather Review*, 112(12):2479 – 2498.

Weisman, M. L. and Klemp, J. B. (1986). *Characteristics of Isolated Convective Storms*, pages 331–358. American Meteorological Society, Boston, MA.

Weusthoff, T. (2011). Weather Type Classification at MeteoSwiss. page 48.

Witt, A., Eilts, M. D., Stumpf, G. J., Johnson, J. T., Mitchell, E. D. W., and Thomas, K. W. (1998). An enhanced hail detection algorithm for the wsr-88d. *Weather and Forecasting*, 13(2):286 – 303.

Acknowledgements

My first thanks goes to my supervisor Prof. Dr. Olivia Romppainen-Martus and my co-supervisor Dr. Katharina Schröer. Both encouraged me with many helpful remarks and discussions that increased the quality of my master thesis considerably. Katharina Schröer receives a special thanks for investing so much time for answering all my questions regarding coding and anything else.

My second thanks goes to David Bancroft for improving the quality of my writing and making it more enjoyable to read.

My last thank you goes to my family and friends. They encouraged me when I was at my lowest and always believed in me during these hard times with lots of home office due to COVID-19.

Declaration of consent

on the basis of Article 30 of the RSL Phil.-nat. 18

Name/First Name:	Schwyn Ursina
Registration Number:	16-207-888
Study program:	M. Sc. in Climate Sciences

Bachelor ☐ Master ☑ Dissertation ☐

Title of the thesis:	Hail occurrence in the Napf region
Supervisor:	Prof. Dr. Olivia Romppainen-Martius

I declare herewith that this thesis is my own work and that I have not used any sources other than those stated. I have indicated the adoption of quotations as well as thoughts taken from other authors as such in the thesis. I am aware that the Senate pursuant to Article 36 paragraph 1 litera r of the University Act of 5 September, 1996 is authorized to revoke the title awarded on the basis of this thesis.

For the purposes of evaluation and verification of compliance with the declaration of originality and the regulations governing plagiarism, I hereby grant the University of Bern the right to process my personal data and to perform the acts of use this requires, in particular, to reproduce the written thesis and to store it permanently in a database, and to use said database, or to make said database available, to enable comparison with future theses submitted by others.

Goldau, January 21, 2022

Place/Date

U. Schwyn

Signature